Electronic Supplementary information for

A new $CaCO_3$-template method to synthesize nanoporous manganese oxides hollow structures and their transformation to high-performance $LiMn_2O_4$ cathode for Lithium-ion batteries

By Chunyu Zhu, Genki Saito, Tomohiro Akiyama*

[*] Prof. T. Akiyama, Dr. C. Zhu, Mr. G. Saito
Center for Advanced Research of Energy & Materials, Hokkaido University, Sapporo 060-8628, Japan.
E-mail: takiyama@eng.hokudai.ac.jp (Tomohiro Akiyama)

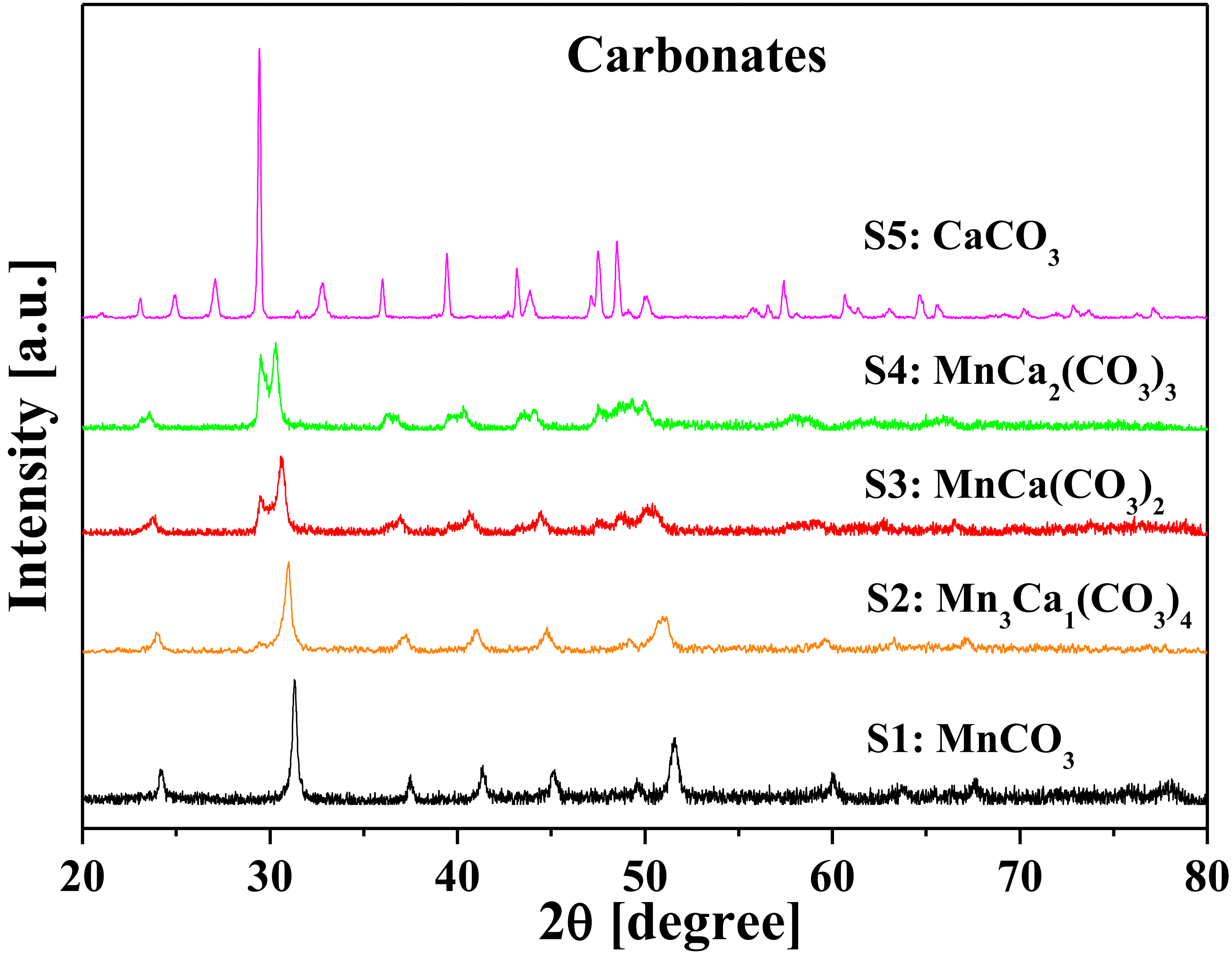

Figure S1. XRD patterns for the coprecipitated carbonates.

Figure S2. SEM images and EDS analysis for the as-prepared carbonates.

(a). S1, $MnCO_3$;

(b). S2, $Mn_3Ca_1(CO_3)_4$;

(c). S3, $Mn_1Ca_1(CO_3)_2$;

(d). S4, $Mn_1Ca_2(CO_3)_3$.

(e). S5, $CaCO_3$

Figure S2-(a)

S1, 1:0, $MnCO_3$

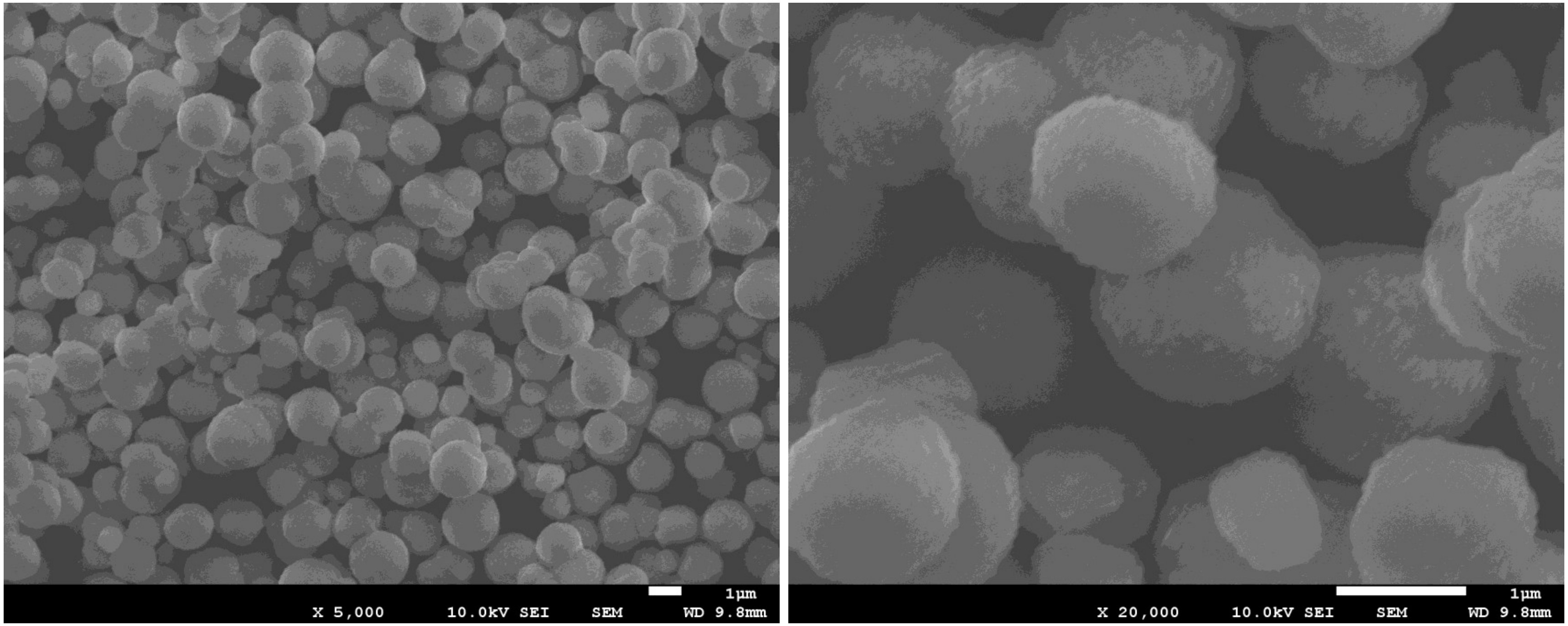

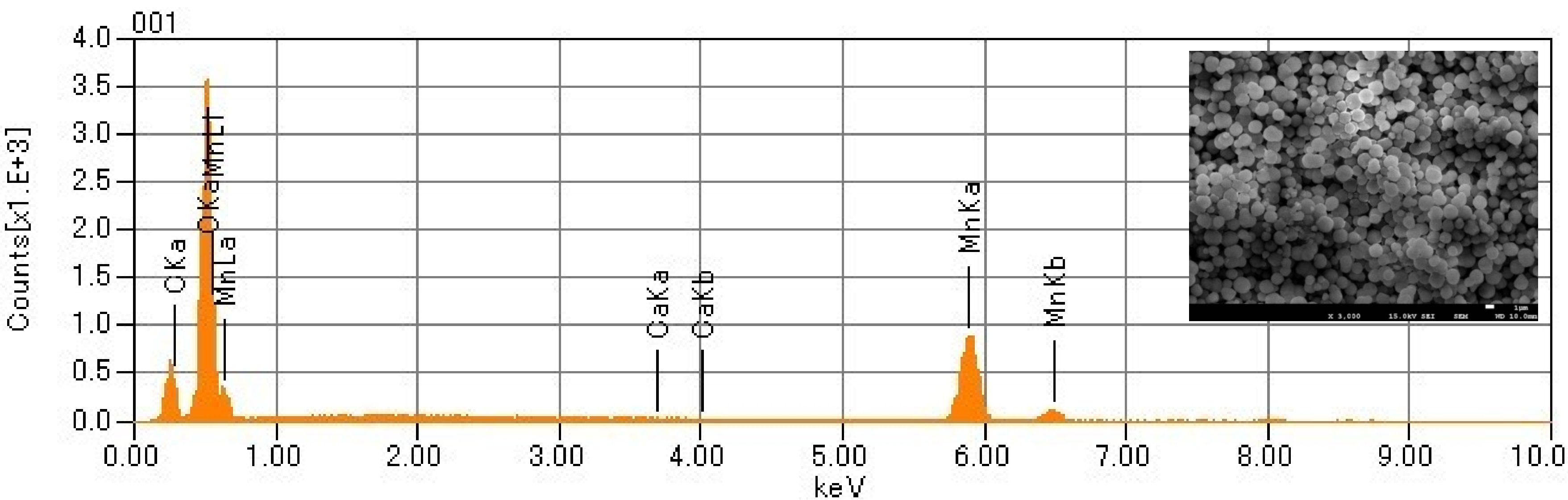

Figure S2-(b)

S2, 3:1, $Mn_3Ca_1(CO_3)_4$

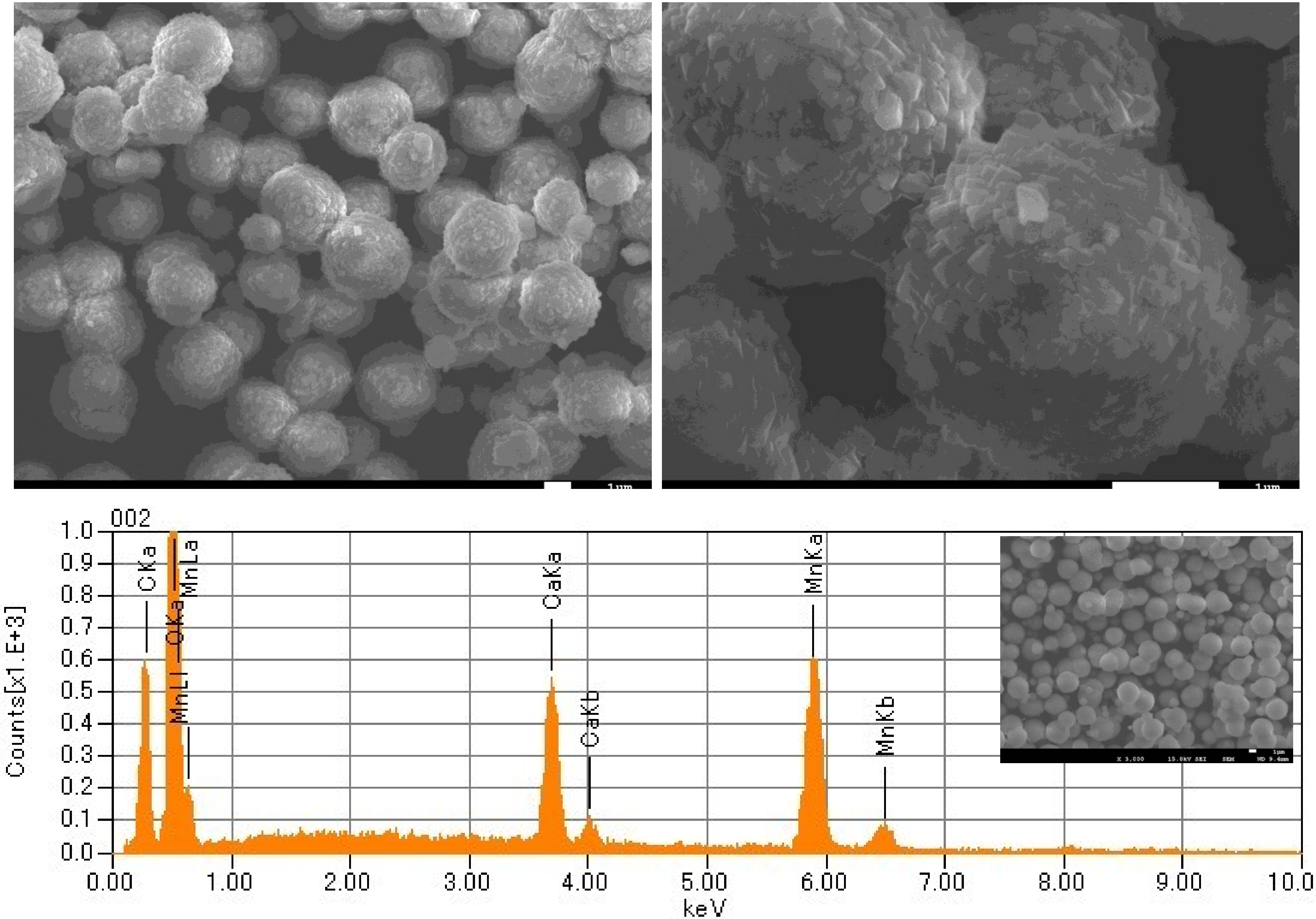

Electronic Supplementary Material (ESI) for Journal of Materials Chemistry A

Figure S2-(c)

S3, 1:1, $Mn_1Ca_1(CO_3)_2$

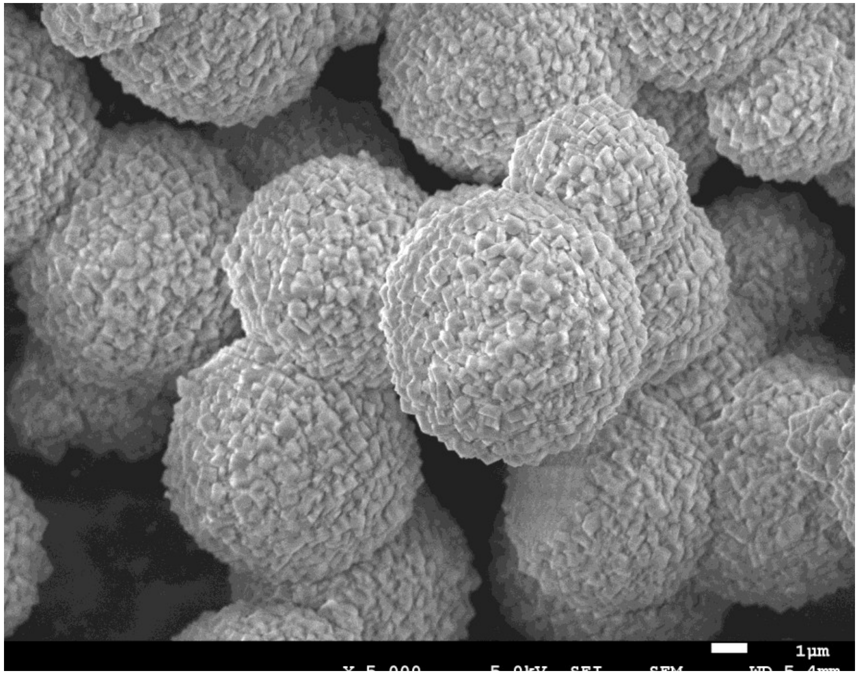

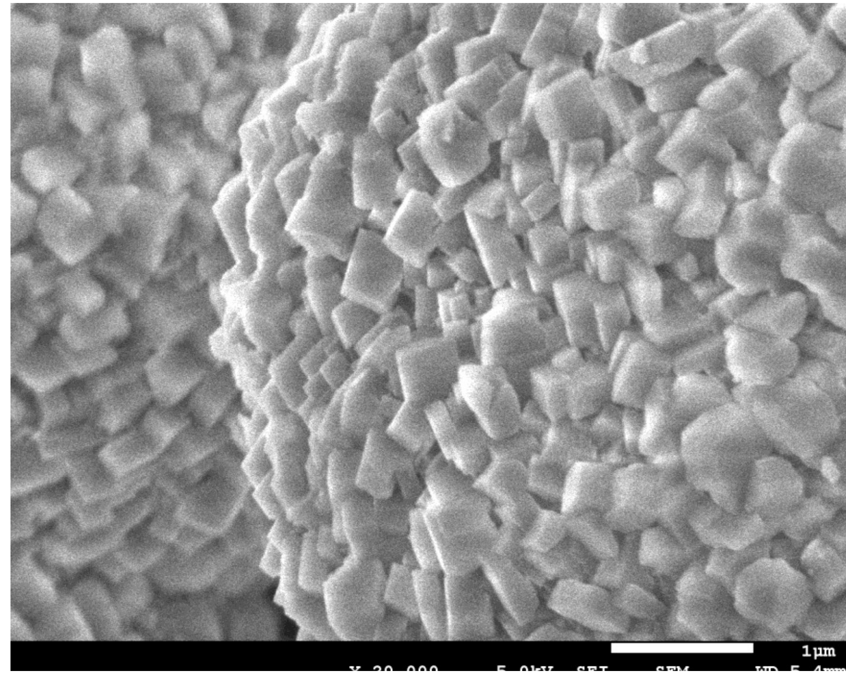

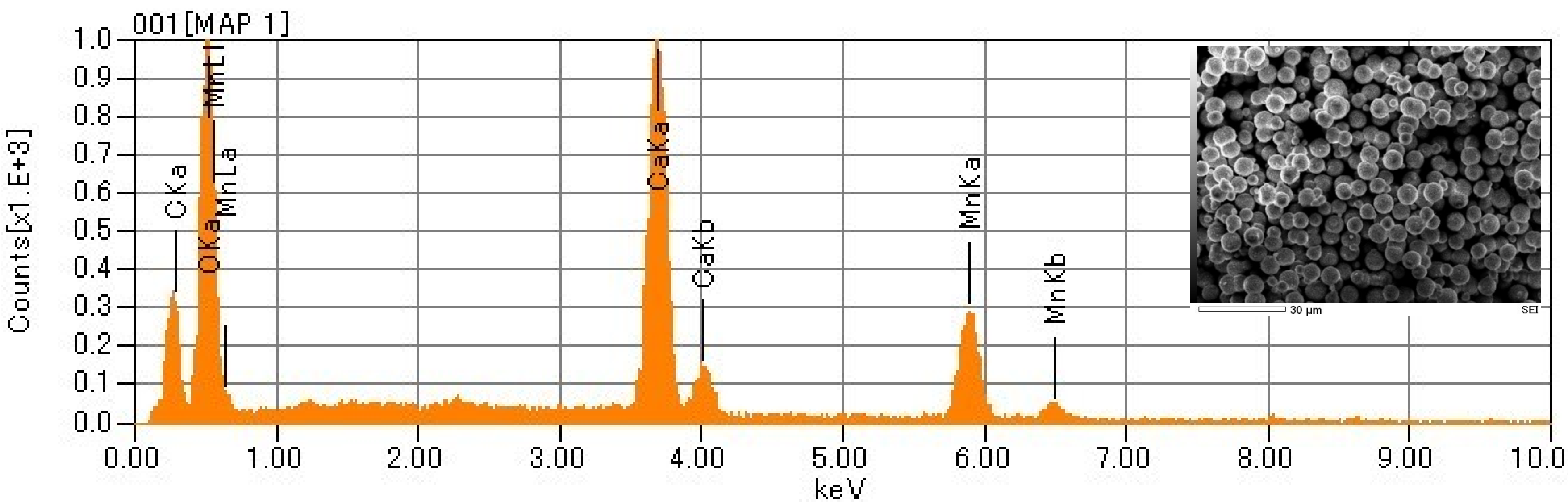

Electronic Supplementary Material (ESI) for Journal of Materials Chemistry A

Figure S2-(d)

S4, 1:2, $Mn_1Ca_2(CO_3)_3$

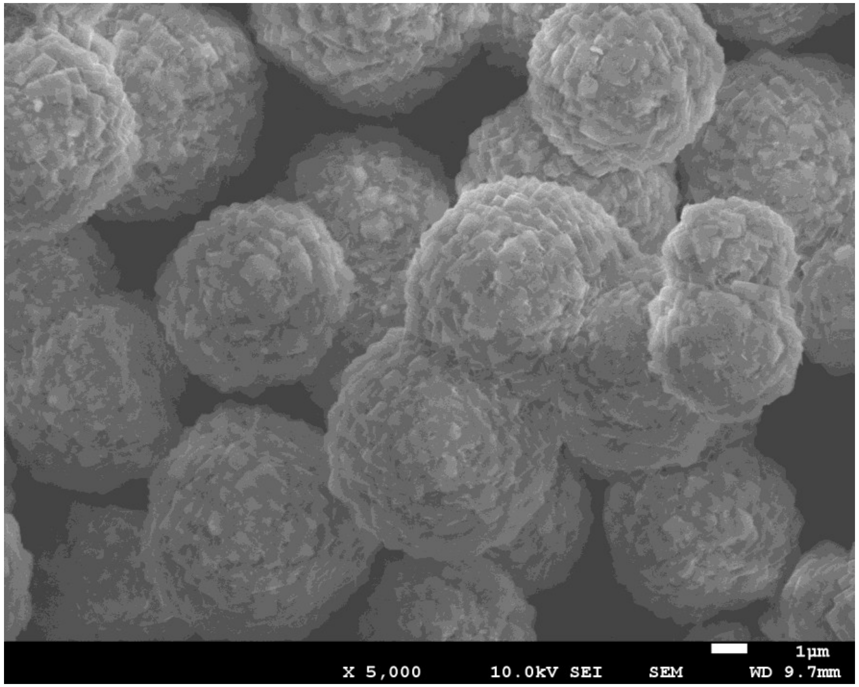

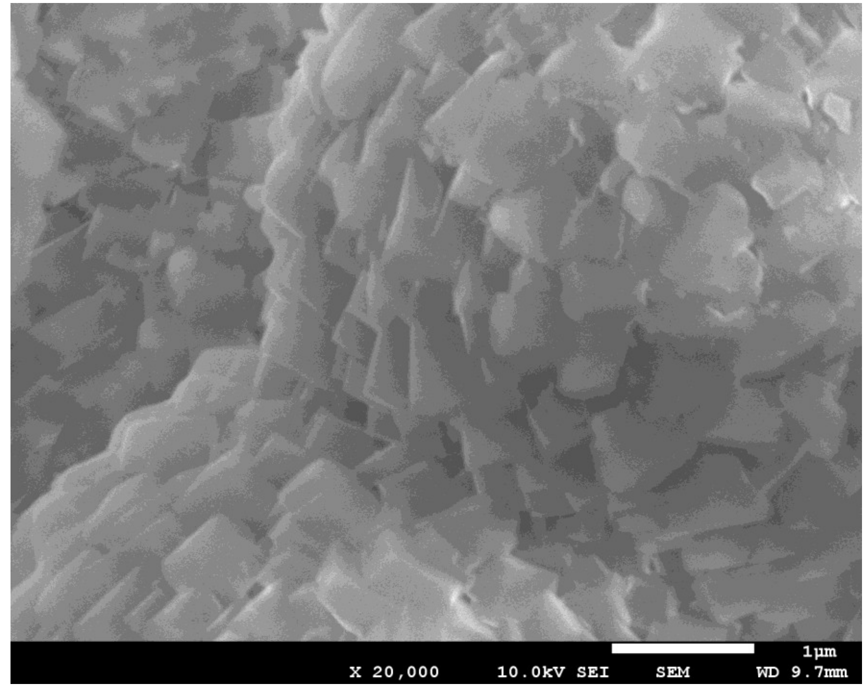

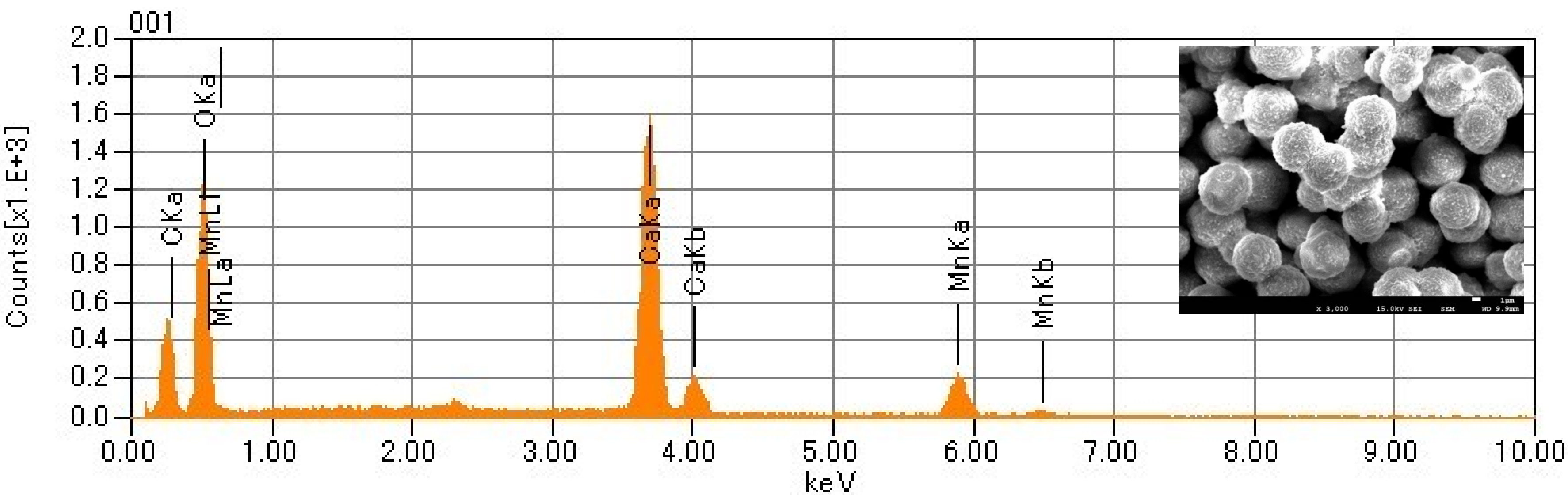

Electronic Supplementary Material (ESI) for Journal of Materials Chemistry A

Figure S2-(e)

S5, $CaCO_3$

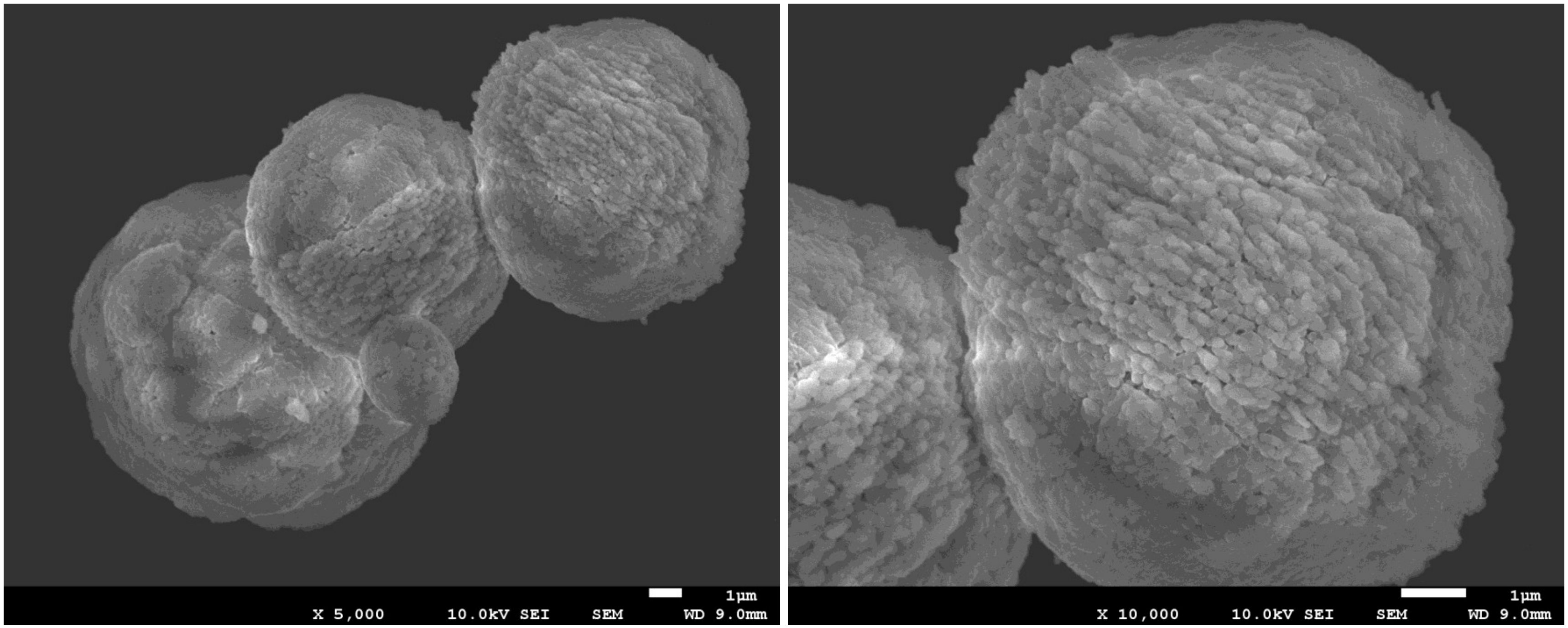

Electronic Supplementary Material (ESI) for Journal of Materials Chemistry A

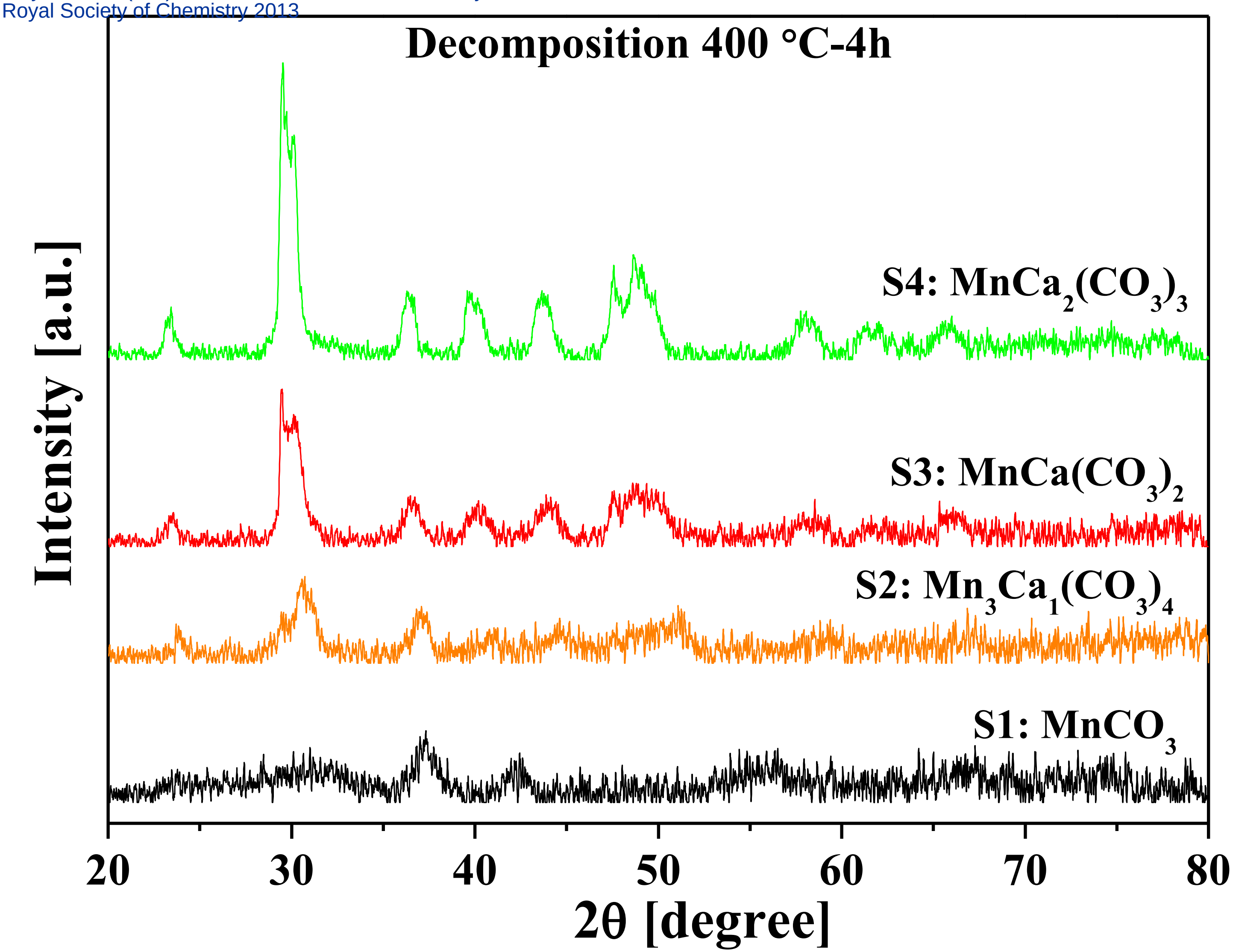

Figure S3. XRD patterns for the carbonates after thermal decomposition at 400 ºC for 4 h.

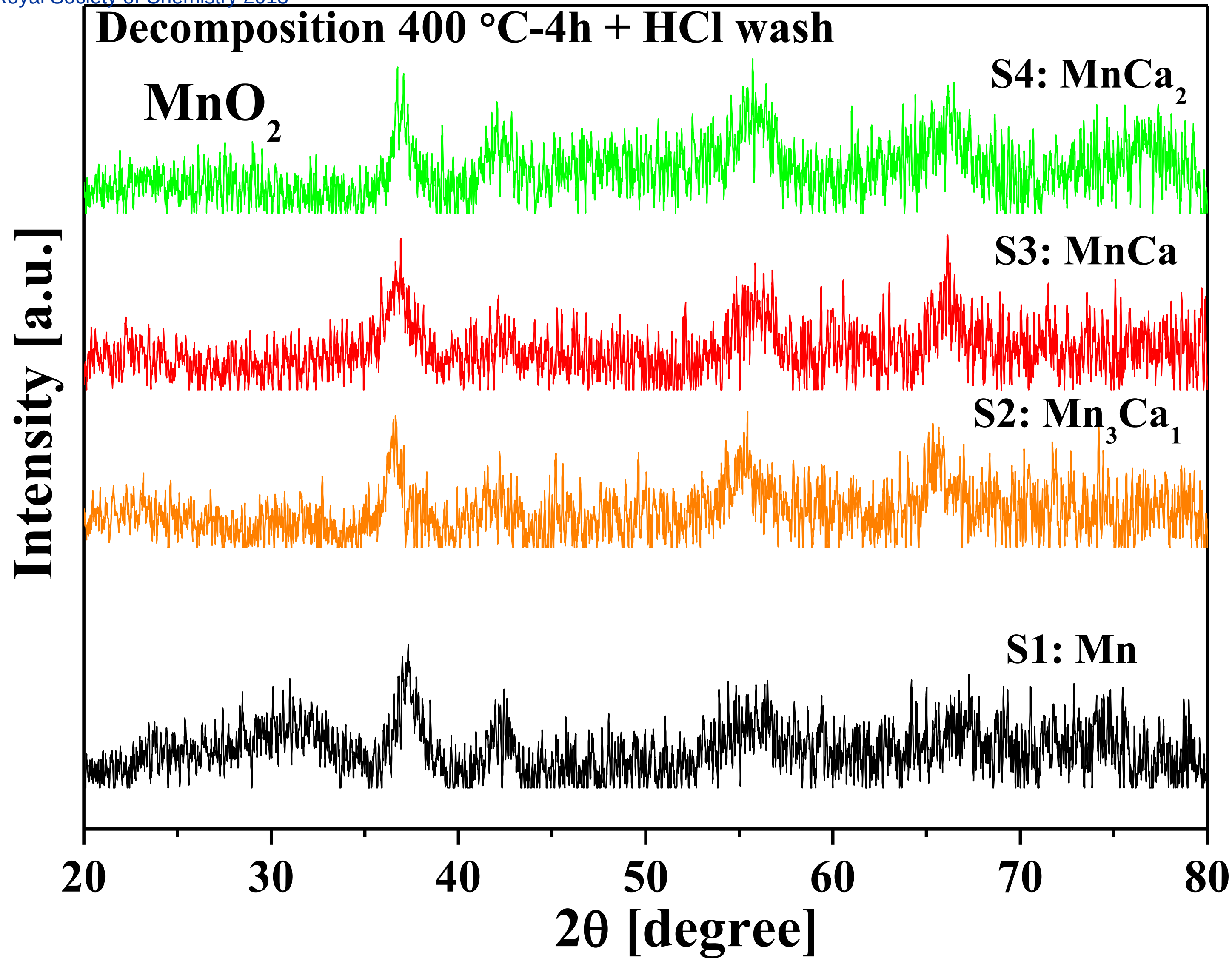

Figure S4. XRD patterns for the carbonates after the treatment of thermal decomposition at 400 ºC for 4 h and HCl wash.

Figure S5. SEM images for the carbonates after thermal decomposition at 400 ºC for 4 h and HCl wash.
(a). S1, from $MnCO_3$, no HCl wash;
(b). S2, from $Mn_3Ca_1(CO_3)_4$;
(c). S3, from $Mn_1Ca_1(CO_3)_2$;
(d). S4, from $Mn_1Ca_2(CO_3)_3$.

Figure S5-(a)

S1, from $MnCO_3$, 400 ºC-4h

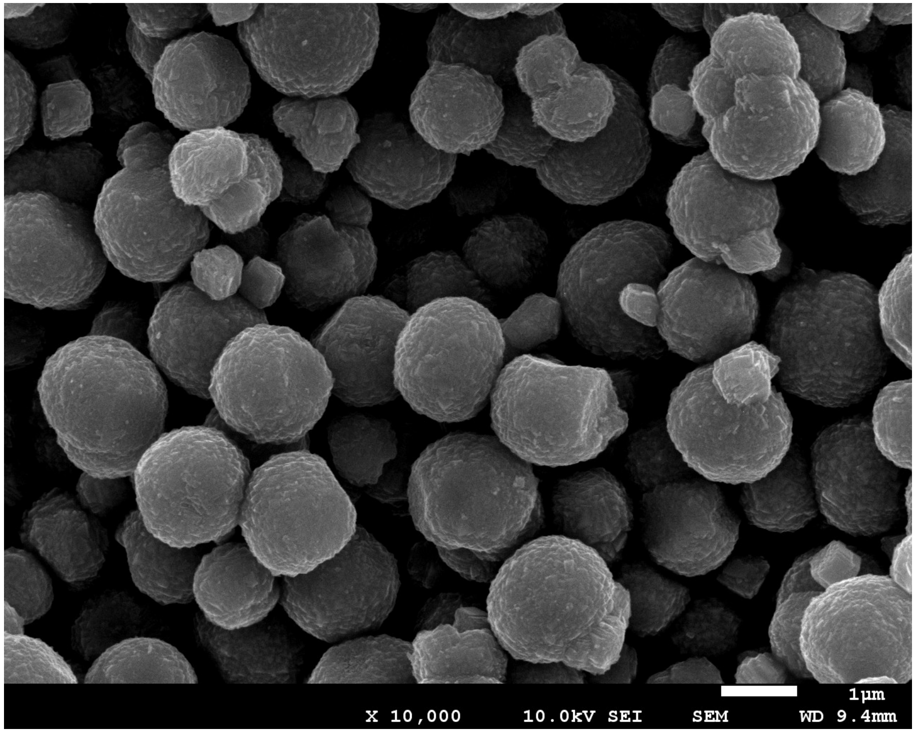

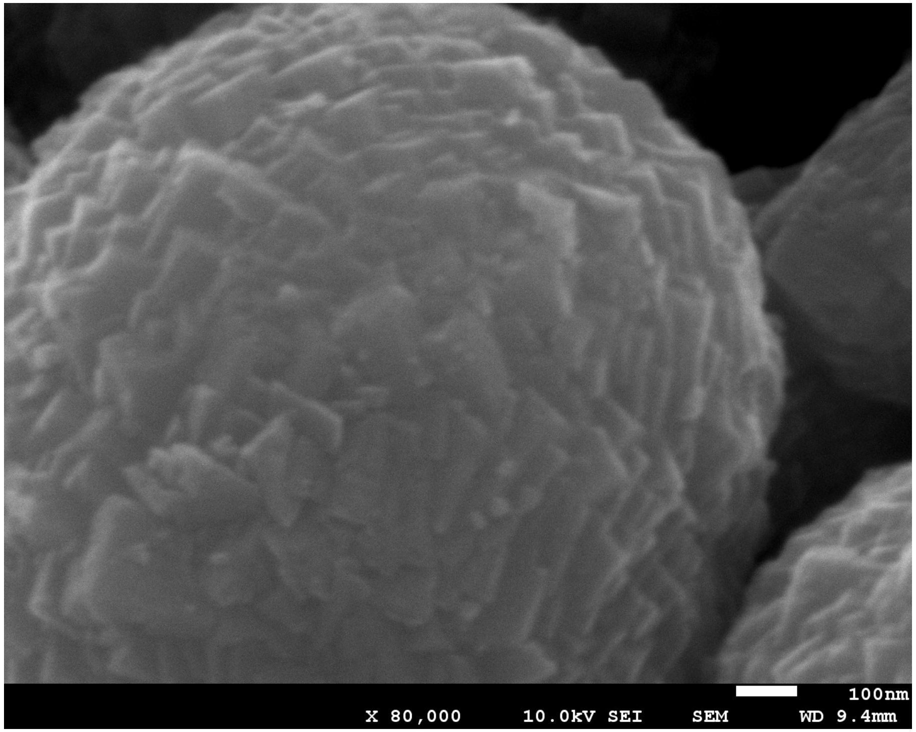

Figure S5-(b) S2, from $Mn_3Ca_1(CO_3)_4$, 400 ºC-4h, HCl wash

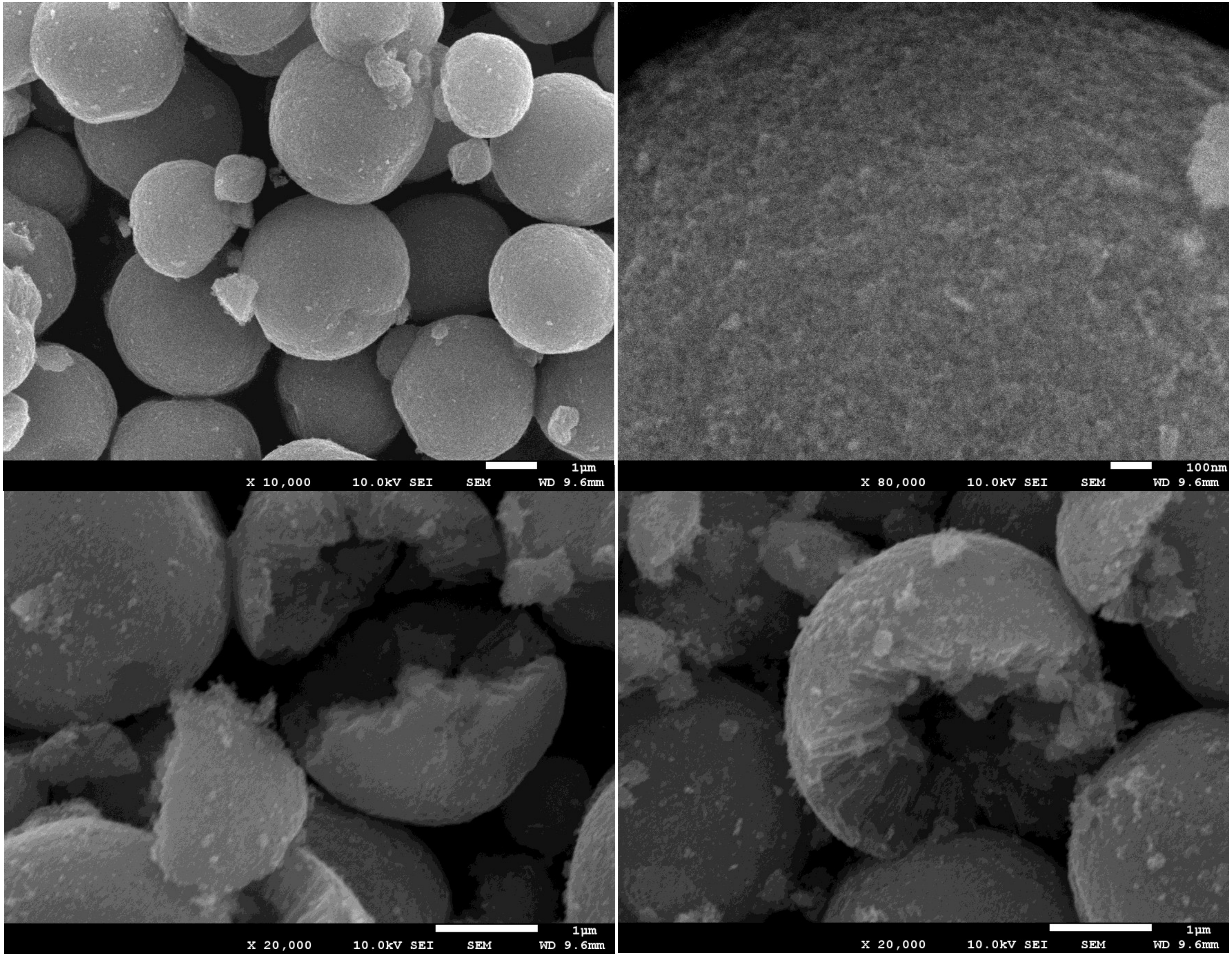

Electronic Supplementary Material (ESI) for Journal of Materials Chemistry A

Figure S5-(c)

S3, from $Mn_1Ca_1(CO_3)_2$, 400 ºC-4h, HCl wash

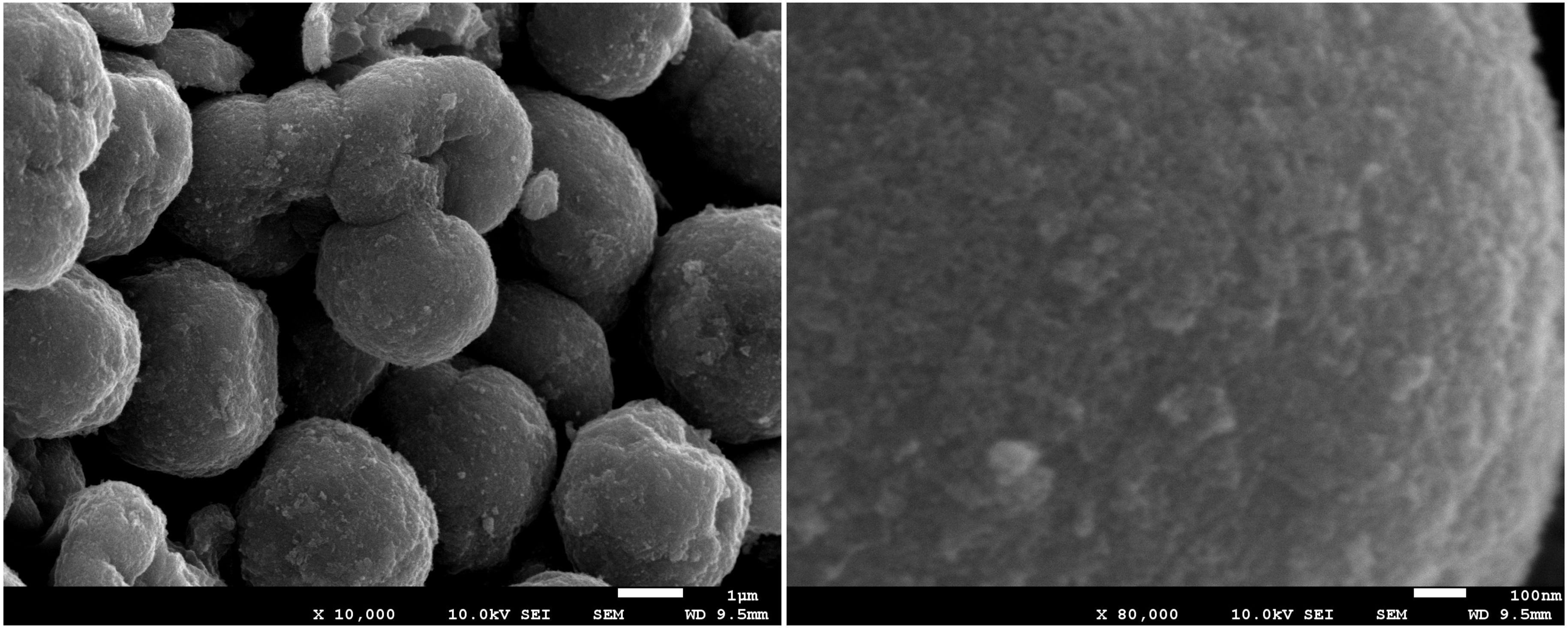

Electronic Supplementary Material (ESI) for Journal of Materials Chemistry A

Figure S5-(d)

S4, from $Mn_1Ca_2(CO_3)_3$, 400 °C-4h, HCl wash

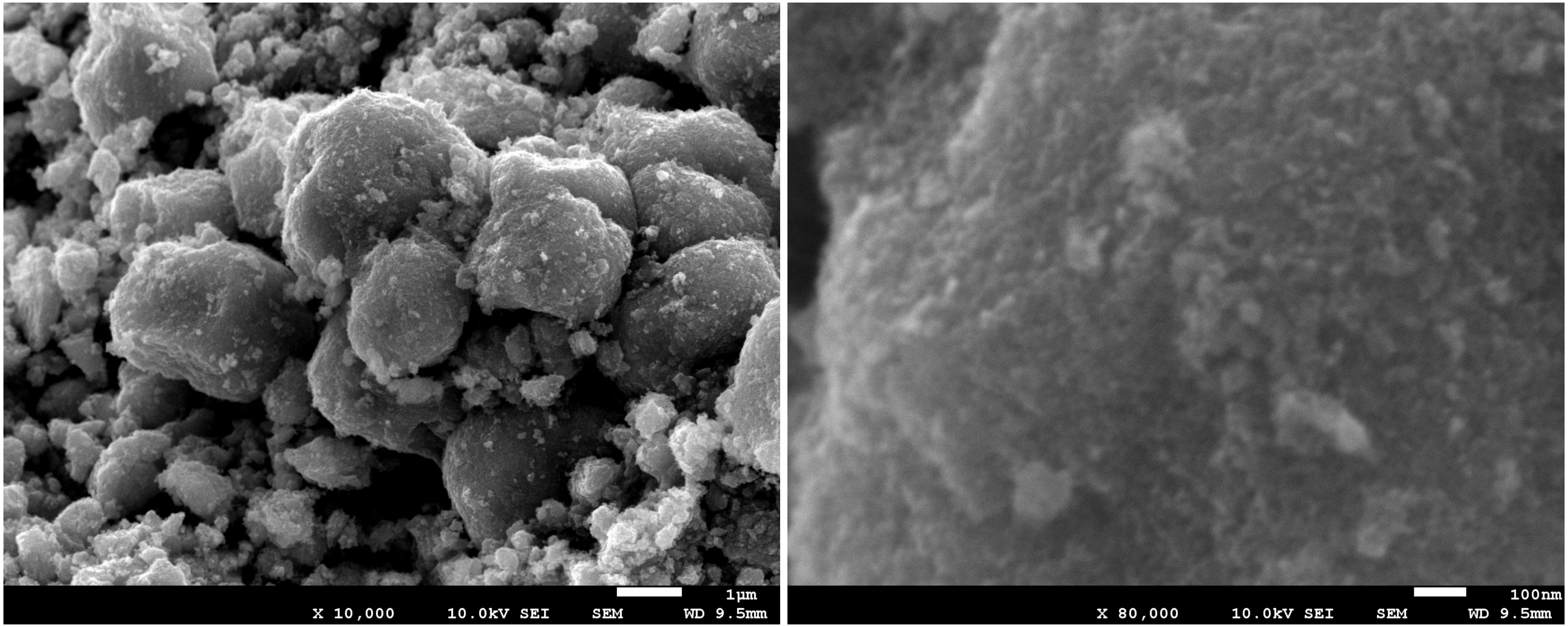

S2, from $Mn_3Ca_1(CO_3)_4$, 400 °C-4h, HCl wash

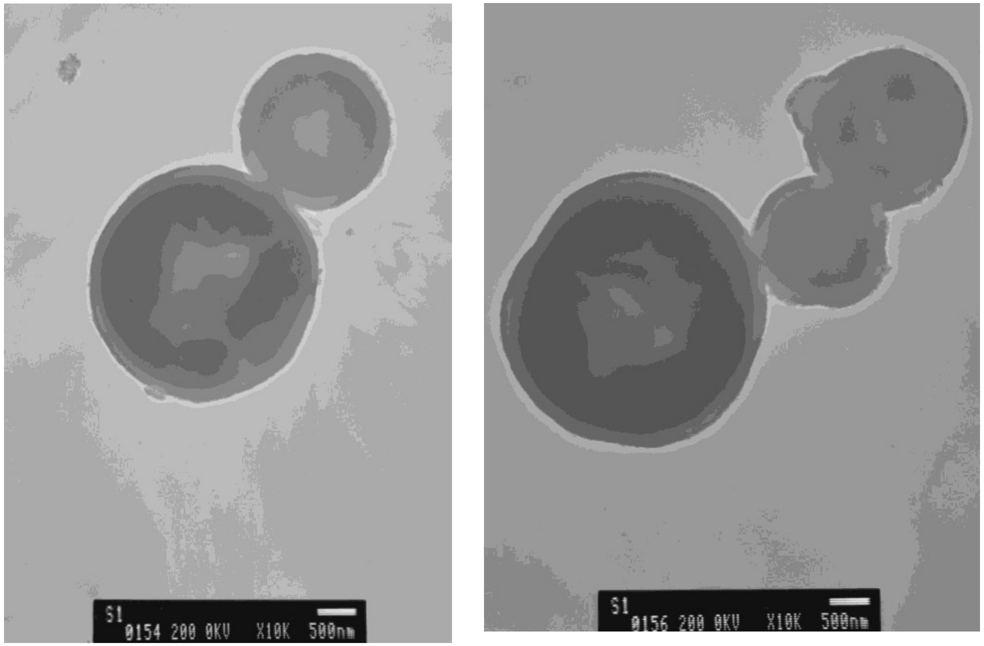

Figure 6. TEM images for the carbonate of $Mn_3Ca_1(CO_3)_4$ after thermal decomposition at 400 °C for 4 h and HCl wash.

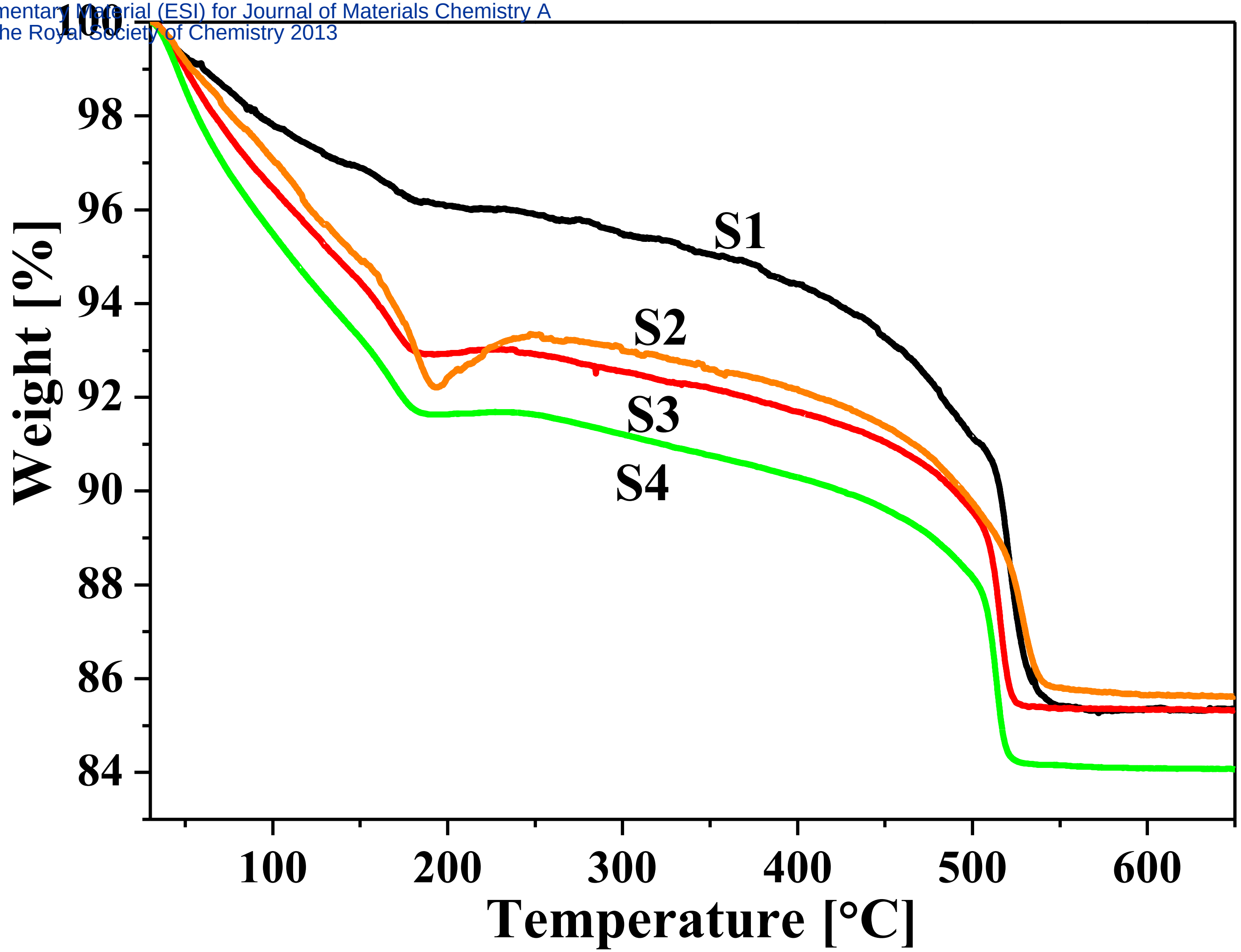

Figure 7. TG curves for the four samples after thermal decomposition at 400 ºC for 4 h and HCl wash. (a). S1, from $MnCO_3$, no HCl wash was used; (b). S2, from $Mn_3Ca_1(CO_3)_4$; (c). S3, from $Mn_1Ca_1(CO_3)_2$; (d). S4, from $Mn_1Ca_2(CO_3)_3$. The analysis were carried out under ambient atmosphere at a heating rate of 5 ºC/min.

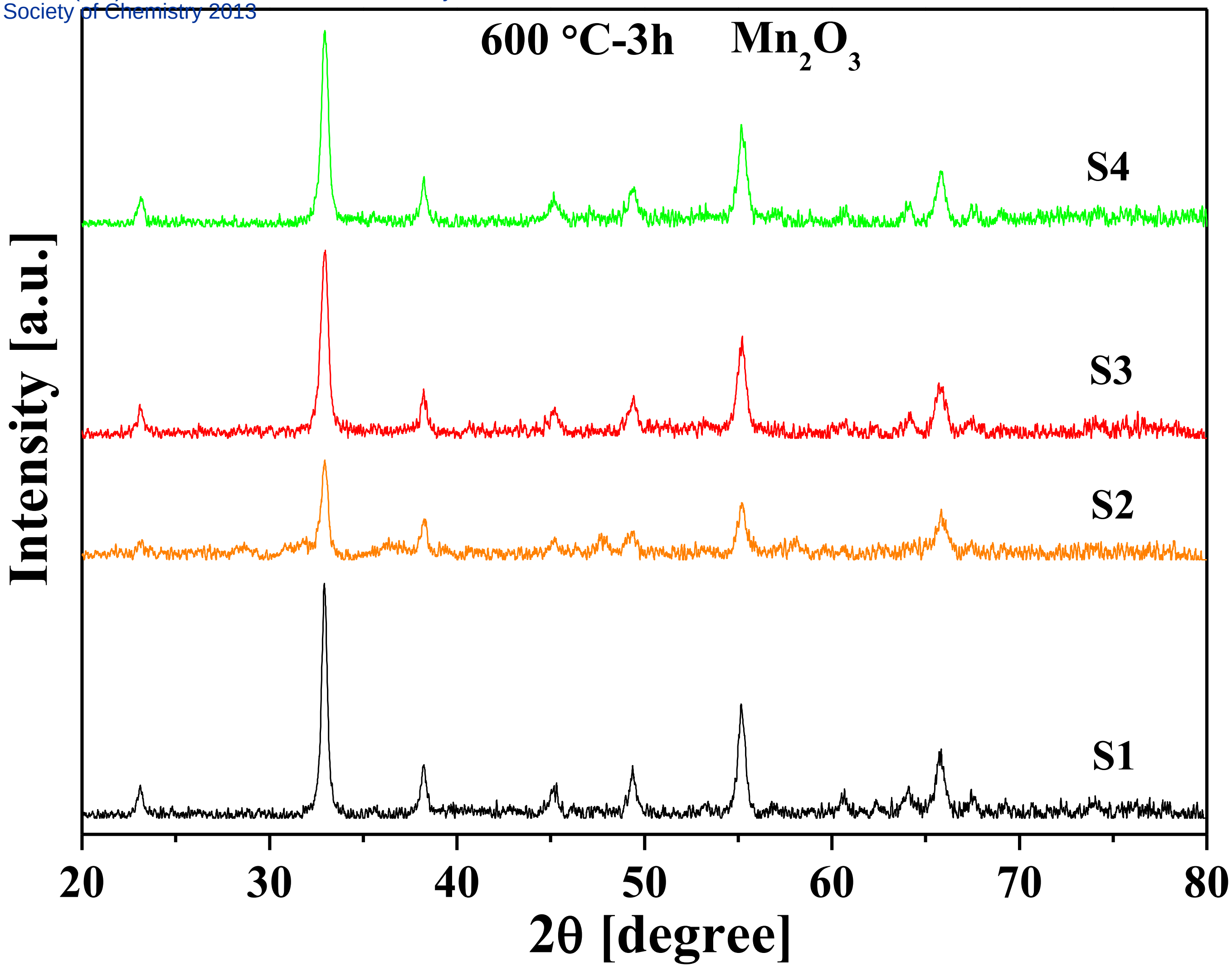

Figure S8. XRD patterns for the carbonates after a series of treatment of thermal decomposition at 400 ºC for 4 h, HCl wash, and thermal decomposition at 600 ºC for 3 h. S1 was obtained by directly decomposition at 600 ºC for 3 h.

Figure S9. SEM images for the carbonates after a series of treatment of thermal decomposition at 400 ^{o}C for 4 h, HCl wash, and thermal decomposition at 600 ^{o}C for 3 h.
(a). S1, from $MnCO_3$, directly decomposed at 600 ^{o}C for 3 h;
(b). S2, from $Mn_3Ca_1(CO_3)_4$;
(c). S3, from $Mn_1Ca_1(CO_3)_2$;
(d). S4, from $Mn_1Ca_2(CO_3)_3$.

Figure S9-(a)

S1, from $MnCO_3$, 600 ºC-3h

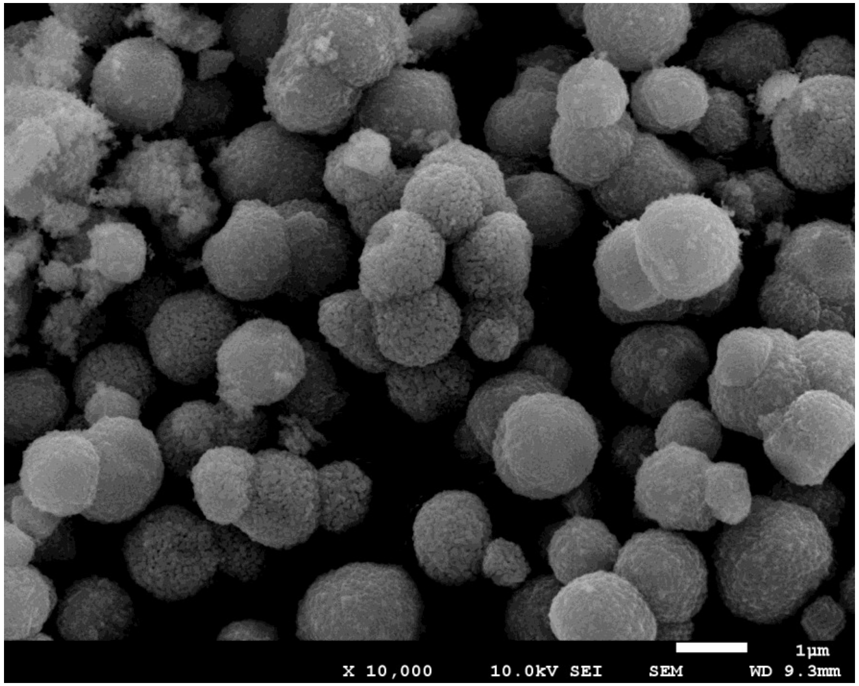

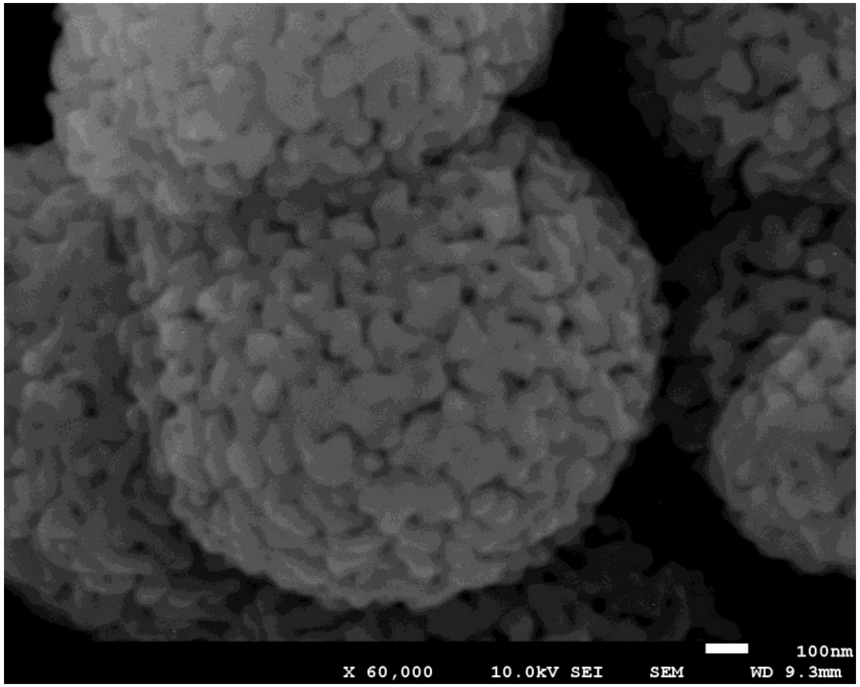

Electronic Supplementary Material (ESI) for Journal of Materials Chemistry A

Figure S9-(b)

S2, from $Mn_3Ca_1(CO_3)_4$, 400 ºC-4h, HCl wash, 600 ºC-3h

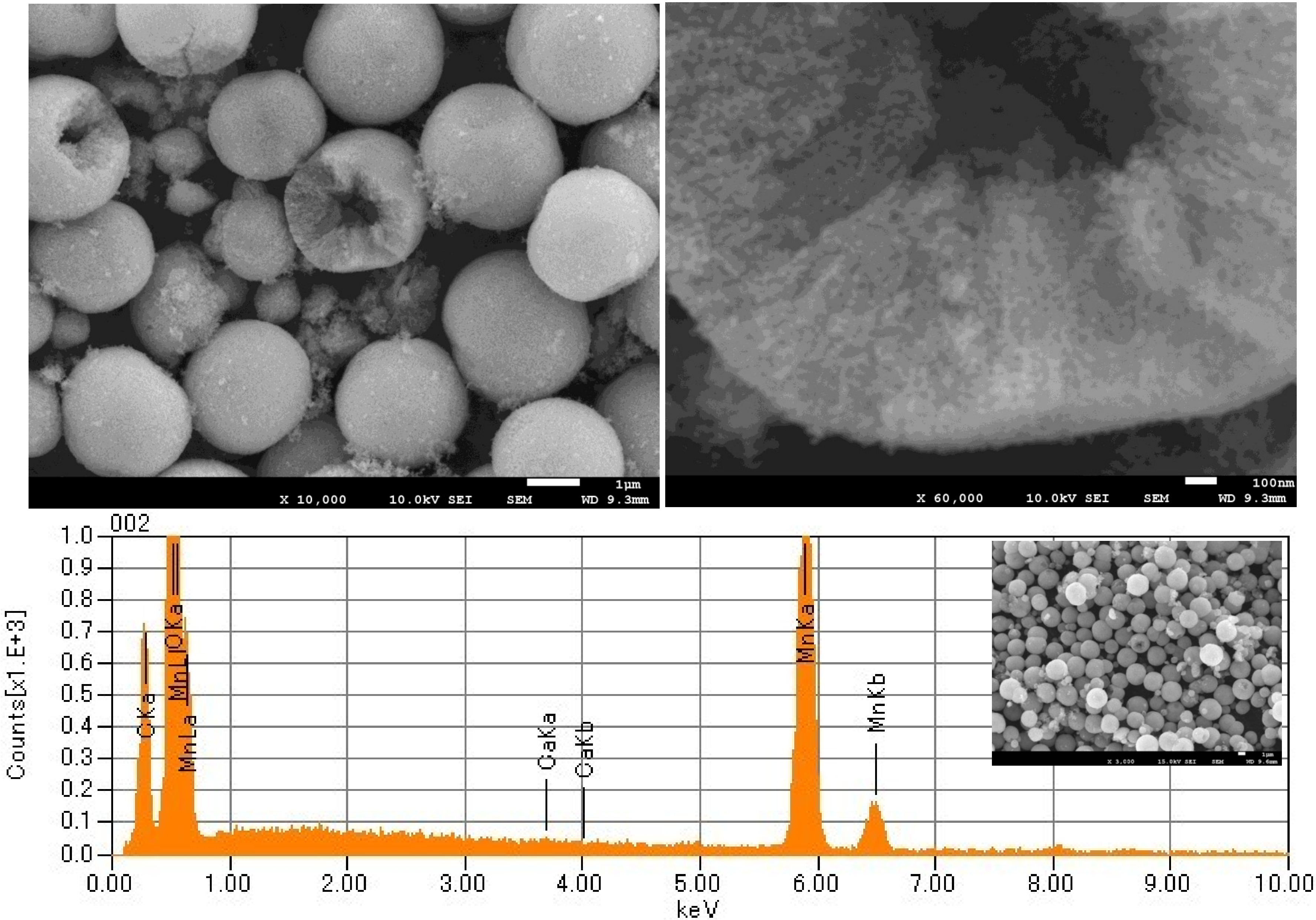

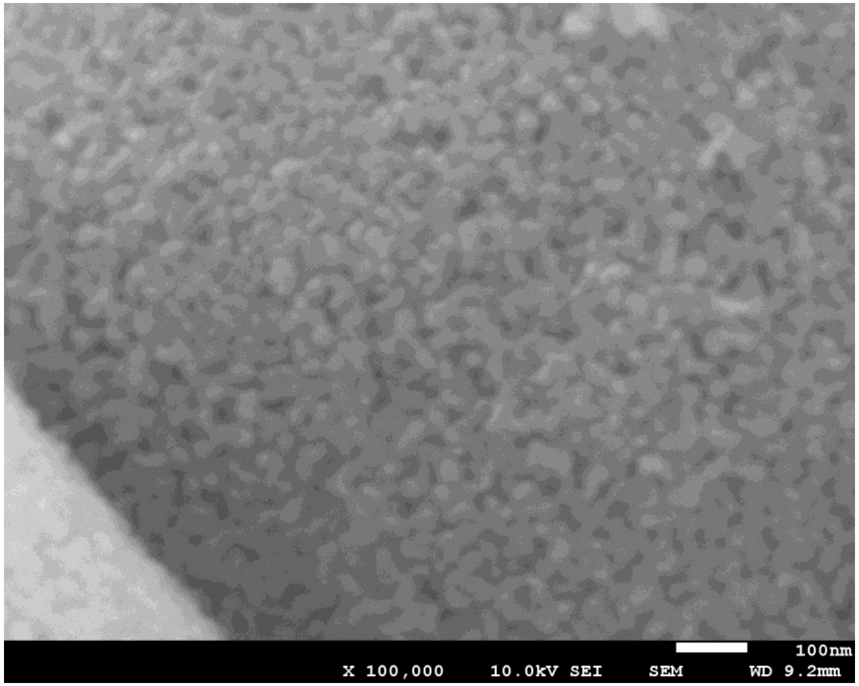
100nm
X 100,000 10.0kV SEI SEM WD 9.2mm

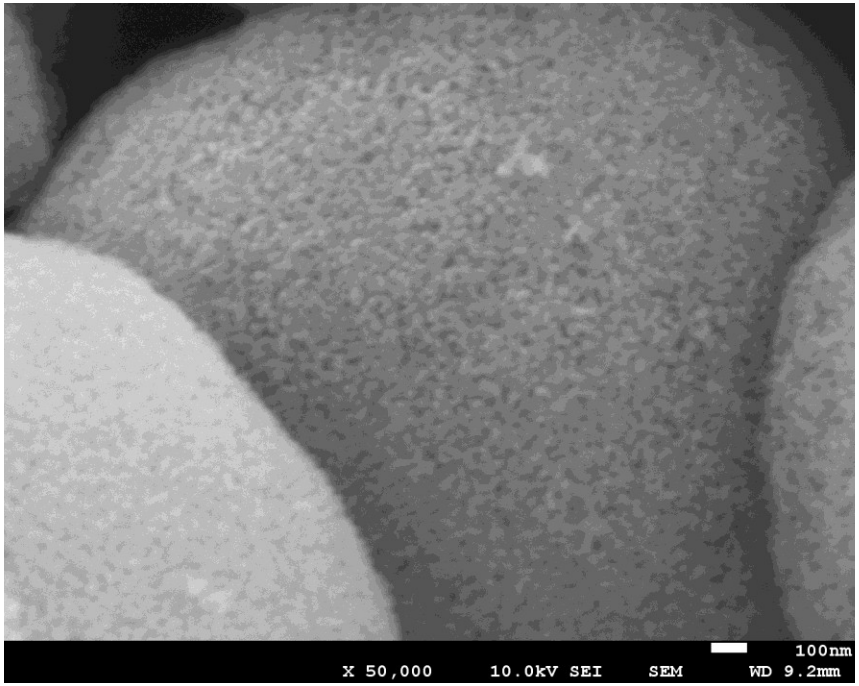
100nm
X 50,000 10.0kV SEI SEM WD 9.2mm

Figure S9-(c) S3, from $Mn_1Ca_1(CO_3)_2$, 400 ºC-4h, HCl wash, 600 ºC-3h

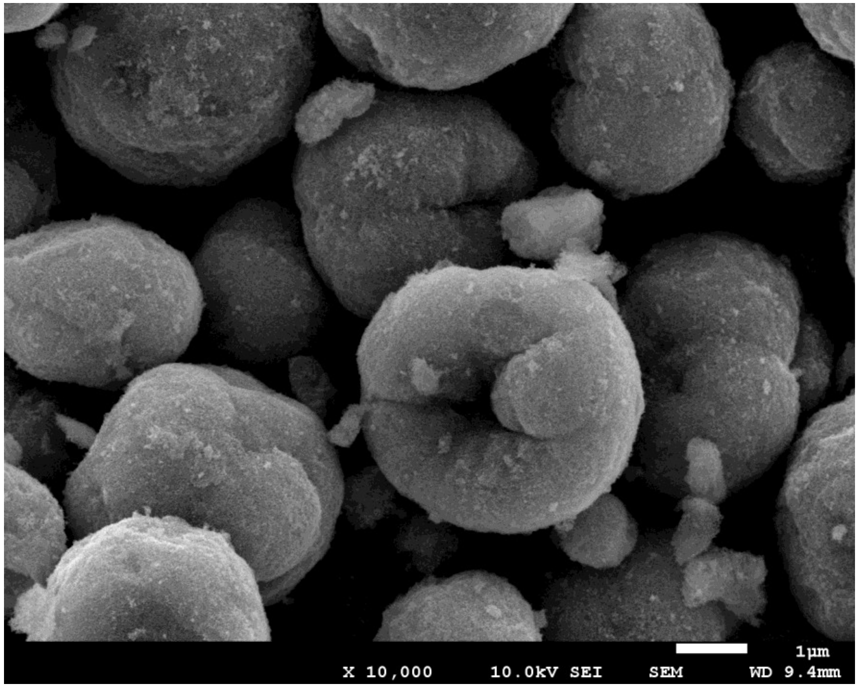

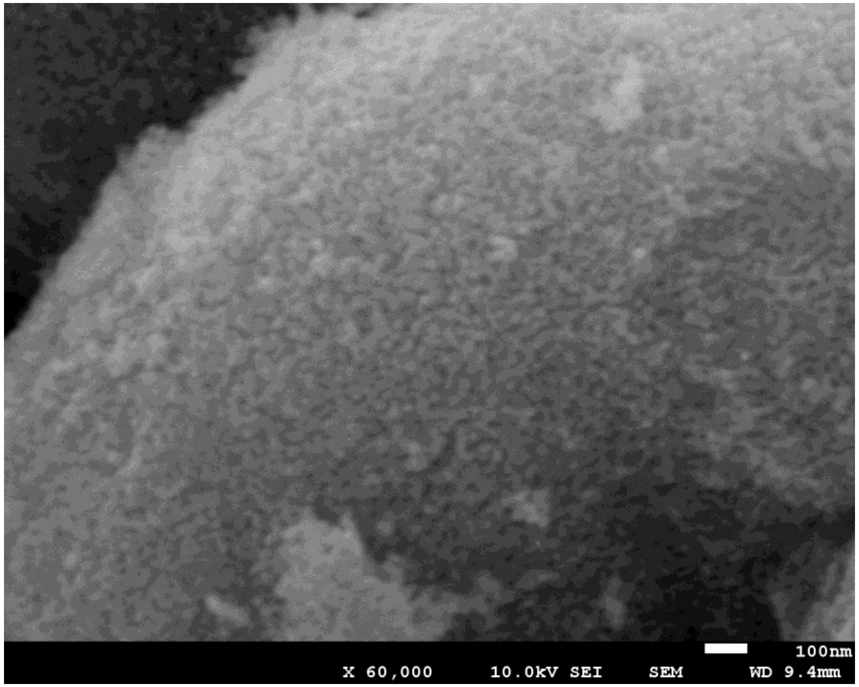

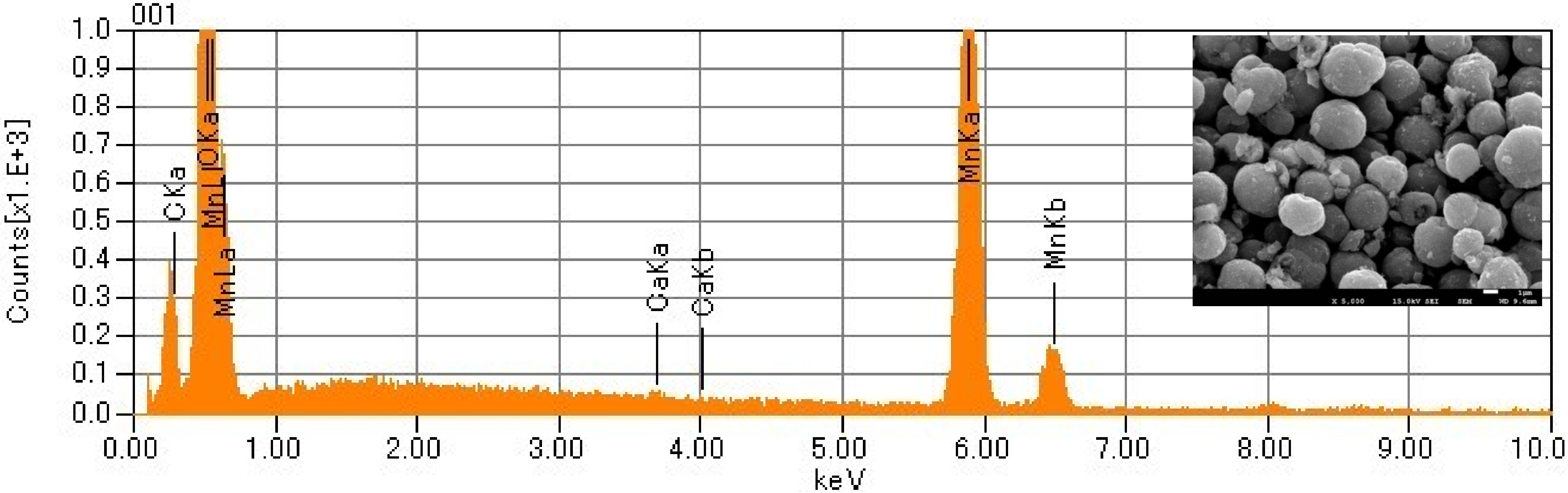

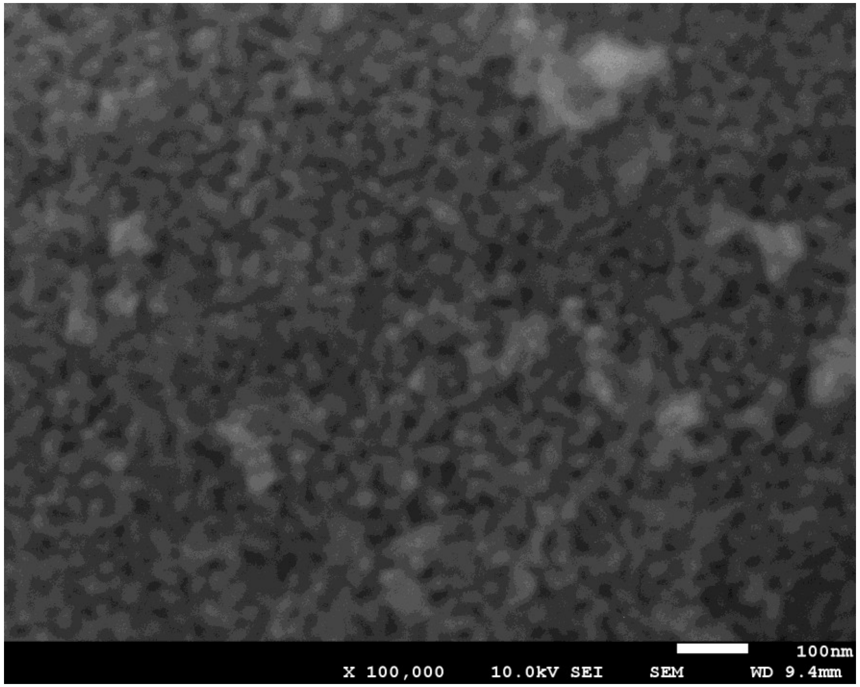
100nm
X 100,000 10.0kV SEI SEM WD 9.4mm

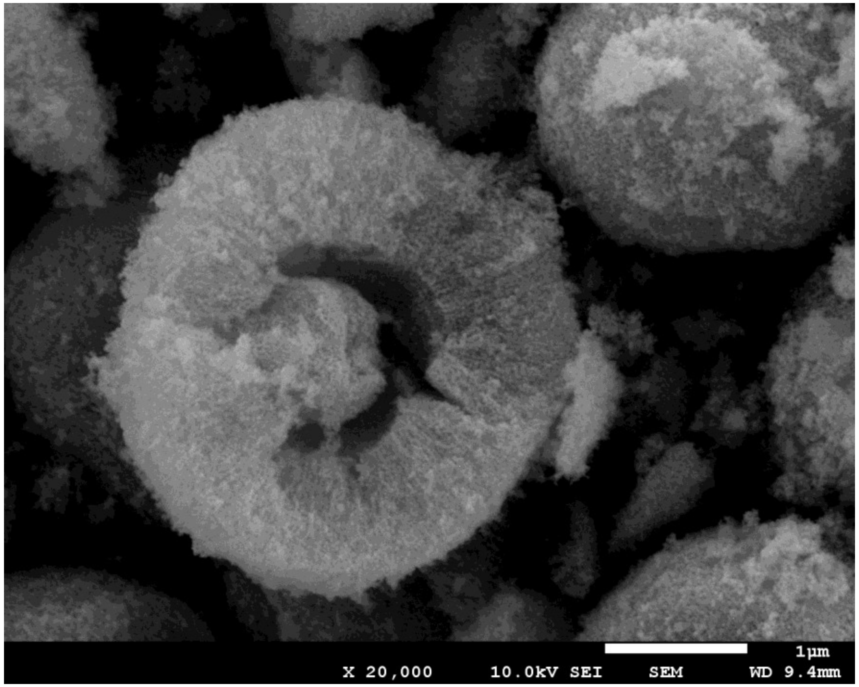
1μm
X 20,000 10.0kV SEI SEM WD 9.4mm

Figure S9-(d) S4, from $Mn_1Ca_2(CO_3)_3$, 400 ºC-4h, HCl wash, 600 ºC-3h

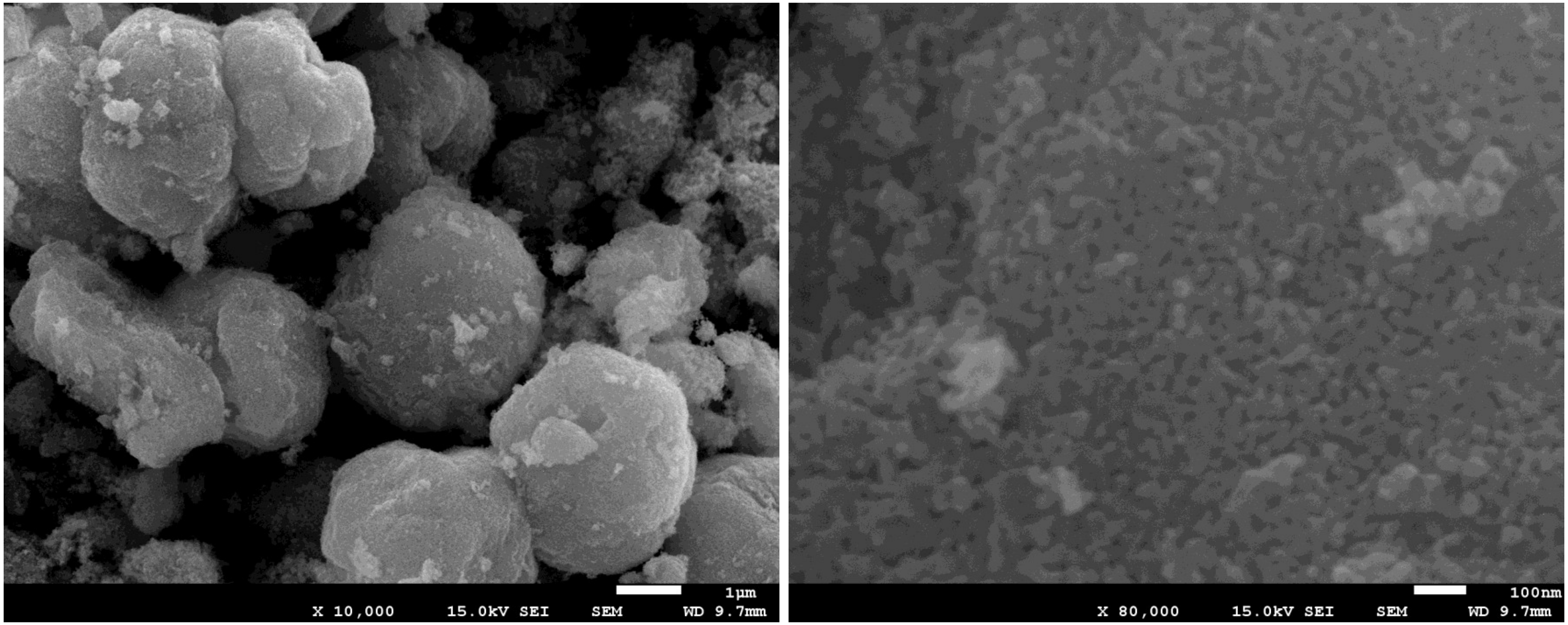

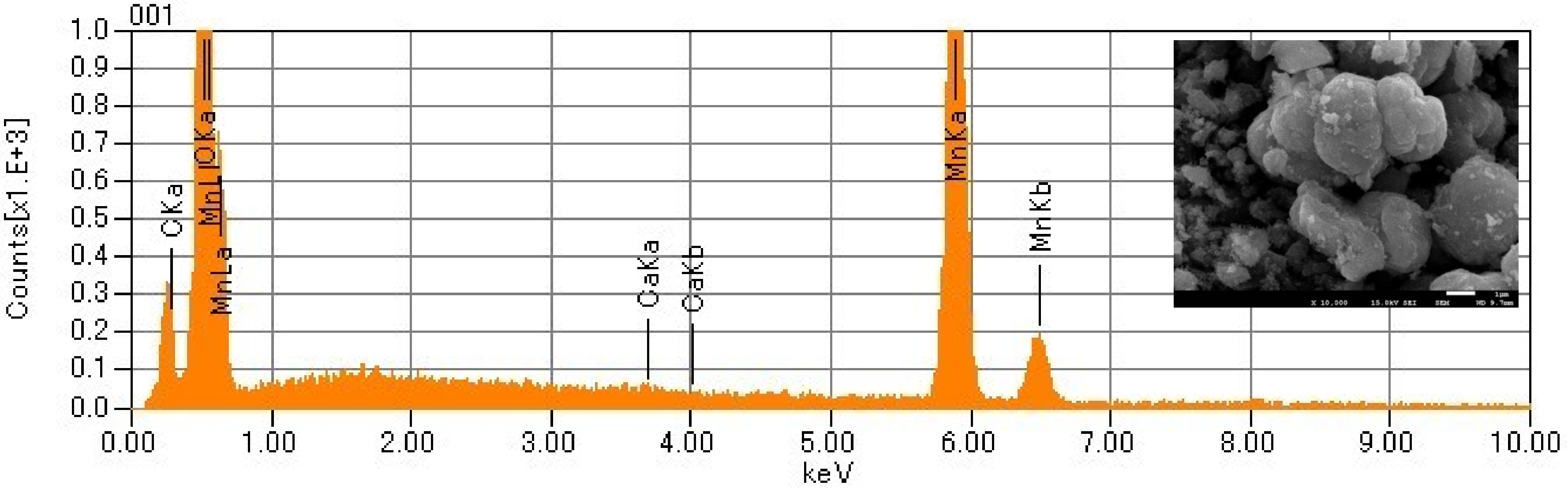

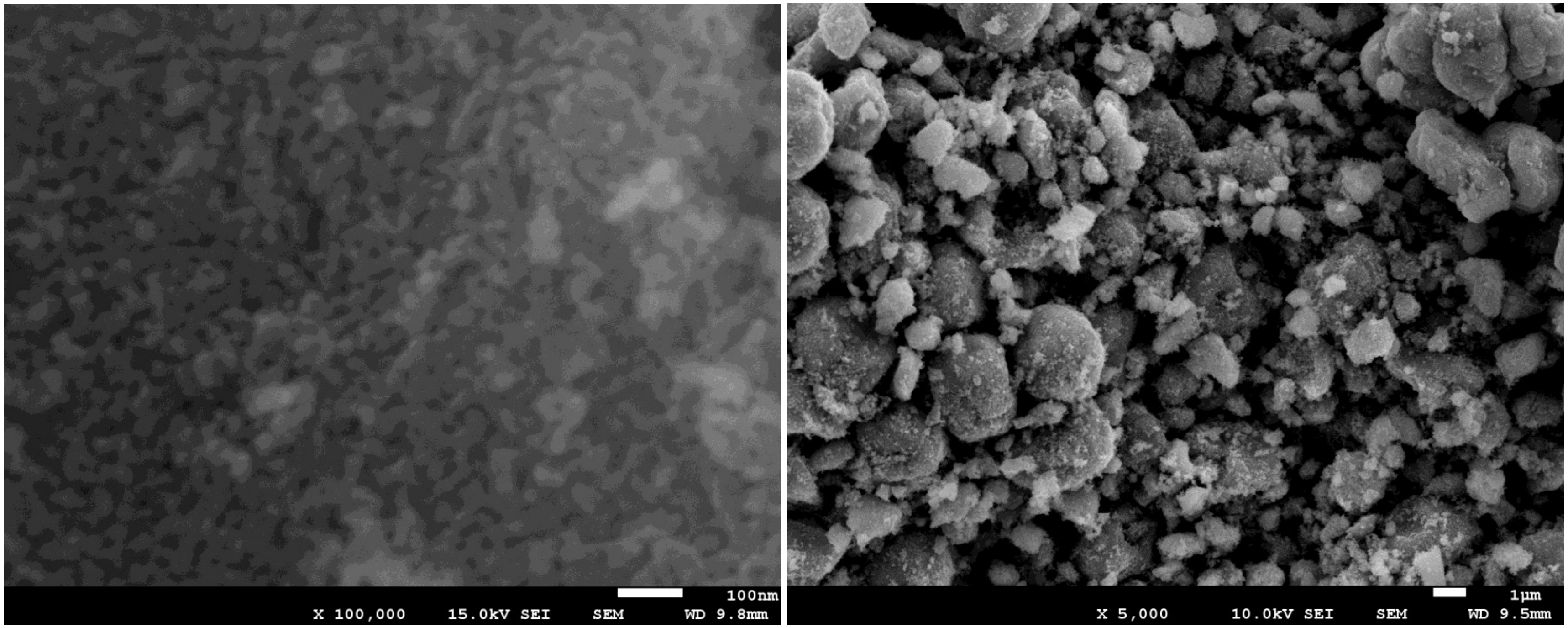
100nm
X 100,000 15.0kV SEI SEM WD 9.8mm
1μm
X 5,000 10.0kV SEI SEM WD 9.5mm

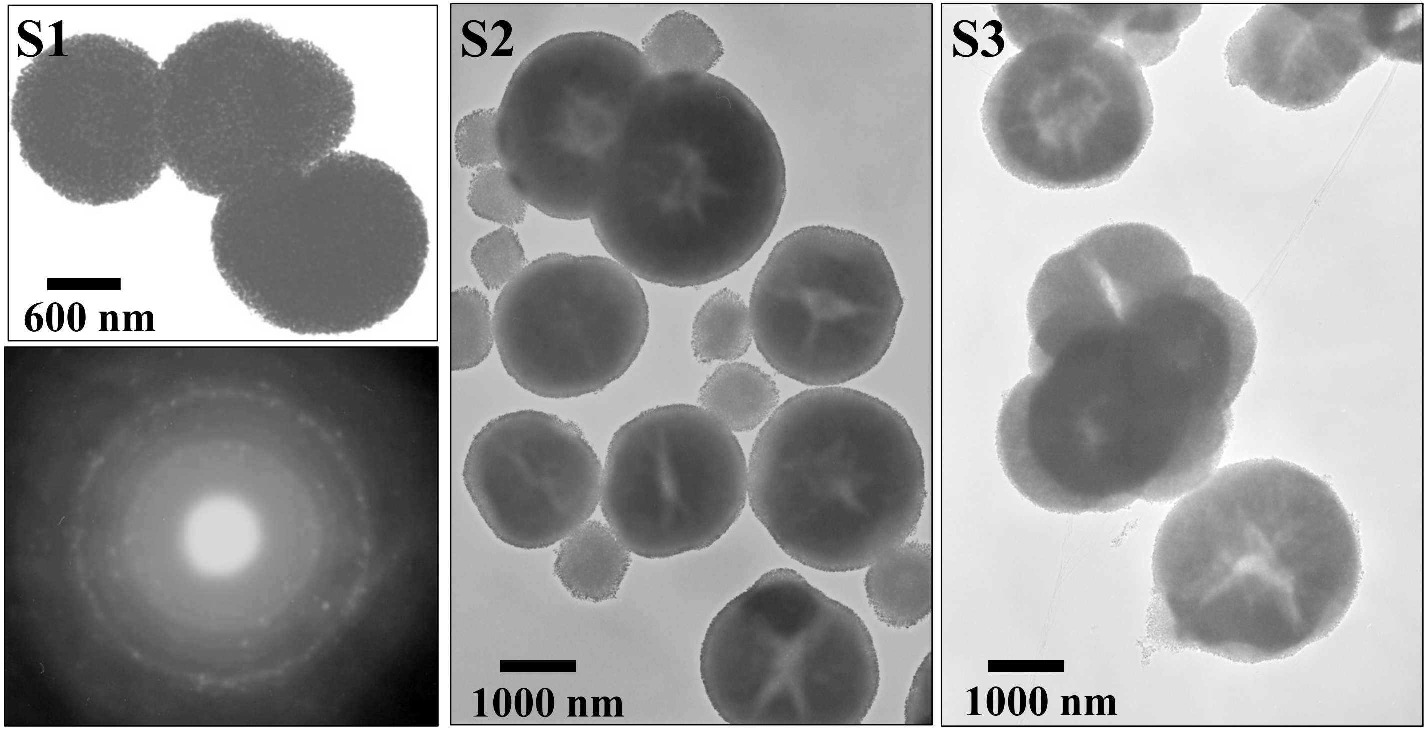

Figure S10. TEM images for the manganese oxide (Mn_2O_3) porous structures obtained from (a). S1, directly from $MnCO_3$ (b). S2, from $Mn_3Ca_1(CO_3)_4$; (c). S3, from $Mn_1Ca_1(CO_3)_2$.

Electronic Supplementary Material (ESI) for Journal of Materials Chemistry A

S1

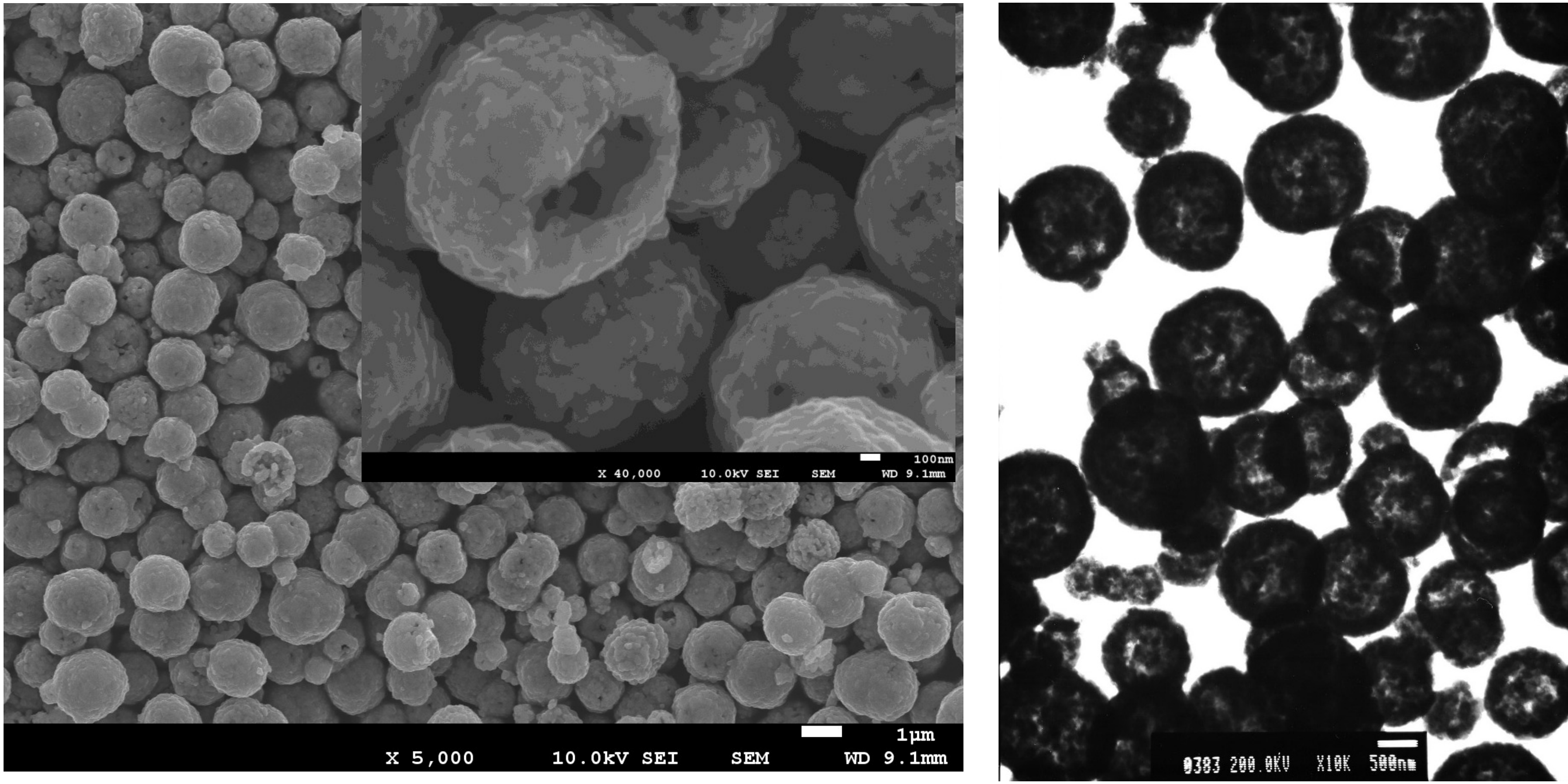

Figure S11. SEM and TEM images for $LiMn_2O_4$ prepared from solid-state reaction of the porous Mn_2O_3 with $LiOH·H_2O$ at 750 ºC for 20 h. S1, porous Mn_2O_3 directly from $MnCO_3$

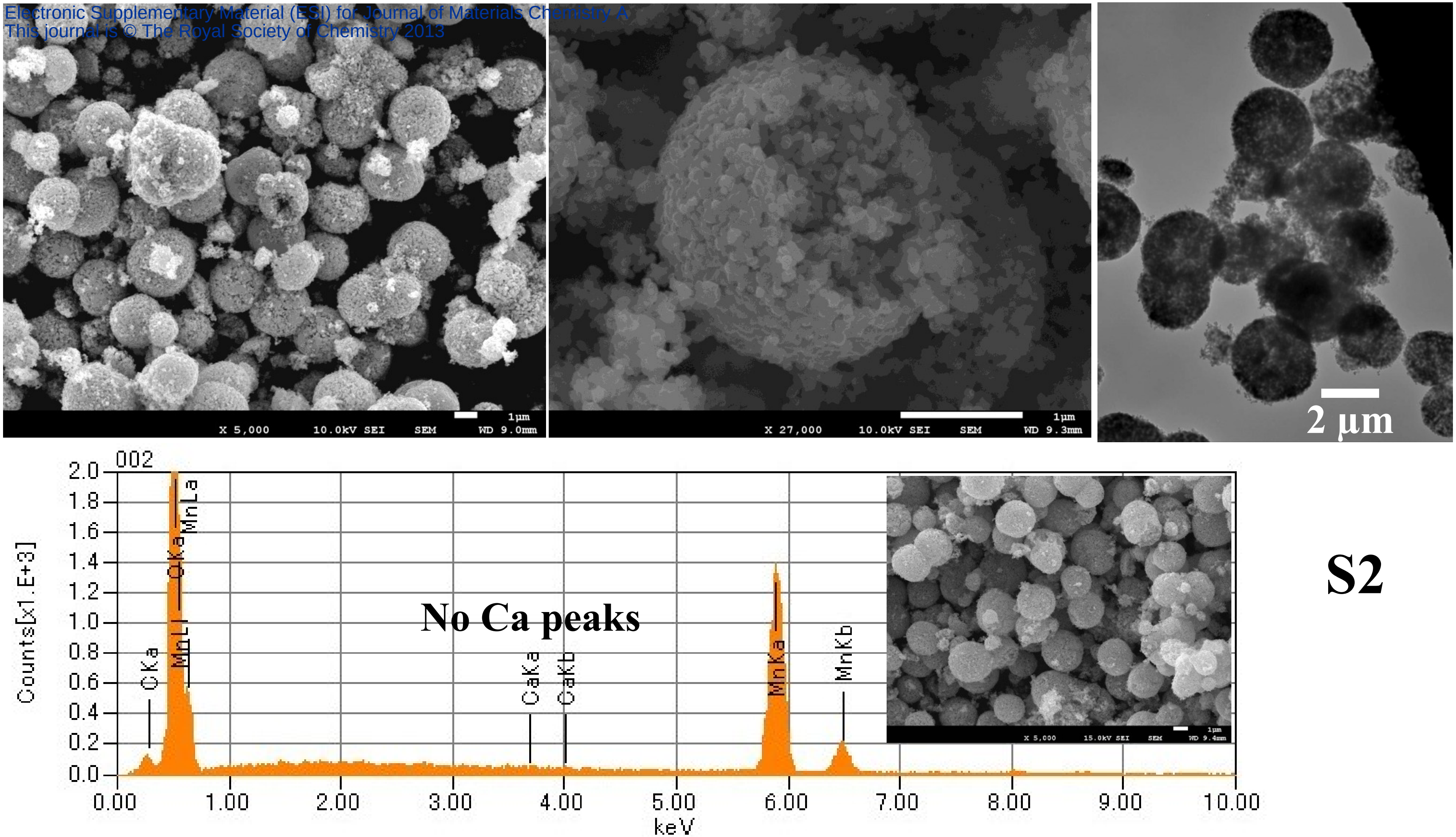

Figure S12. SEM, TEM images and EDS analysis for $LiMn_2O_4$ prepared from solid-state reaction of the porous hollow Mn_2O_3 with $LiOH·H_2O$ at 750 ºC for 20 h. S2, porous Mn_2O_3 hollow spheres from $Mn_3Ca_1(CO_3)_4$.

Electronic Supplementary Material (ESI) for Journal of Materials Chemistry A

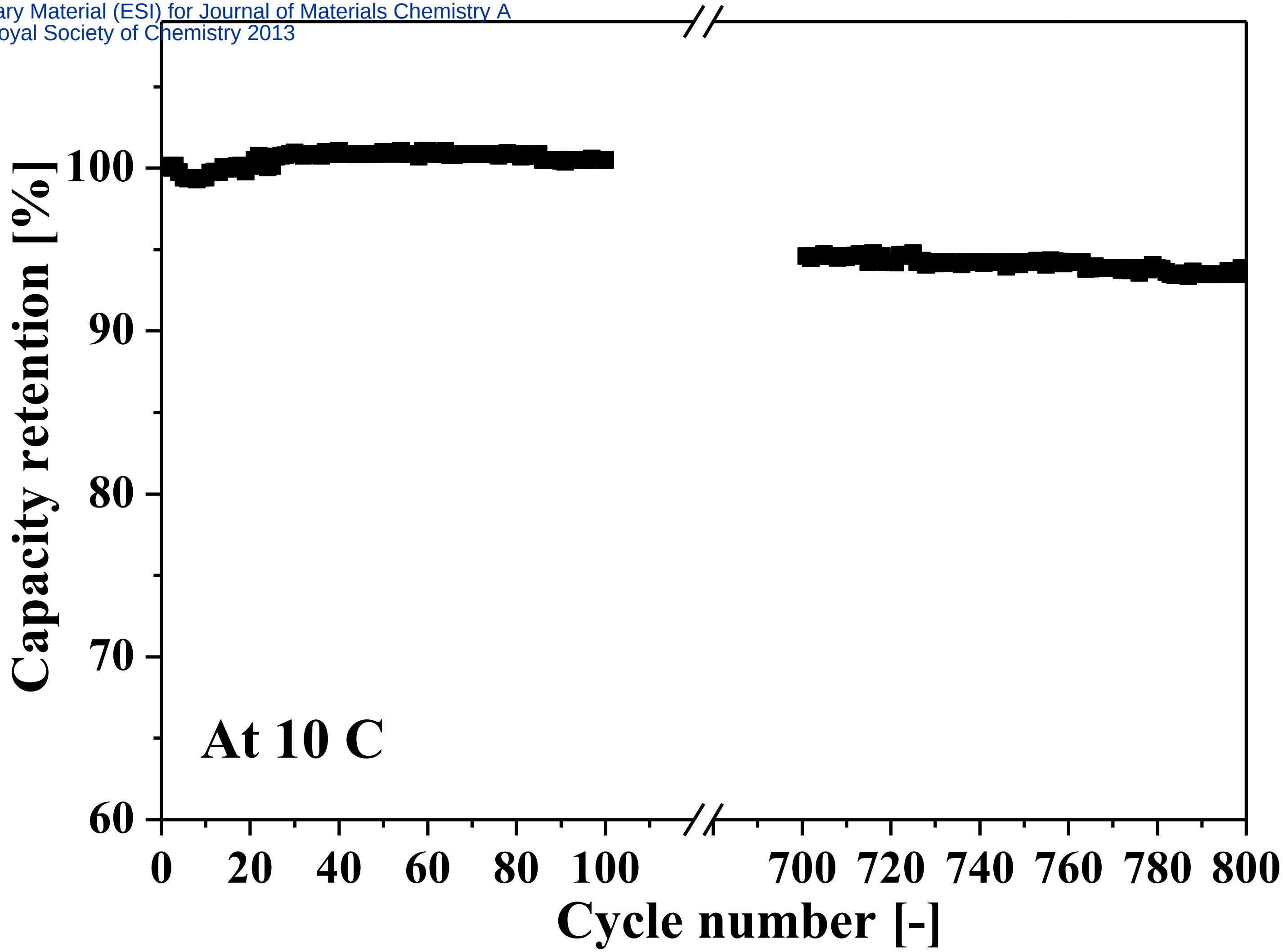

Figure S13. Cycling performance for the porous $LiMn_2O_4$ hollow spheres.

Electronic Supplementary Material (ESI) for Journal of Materials Chemistry A

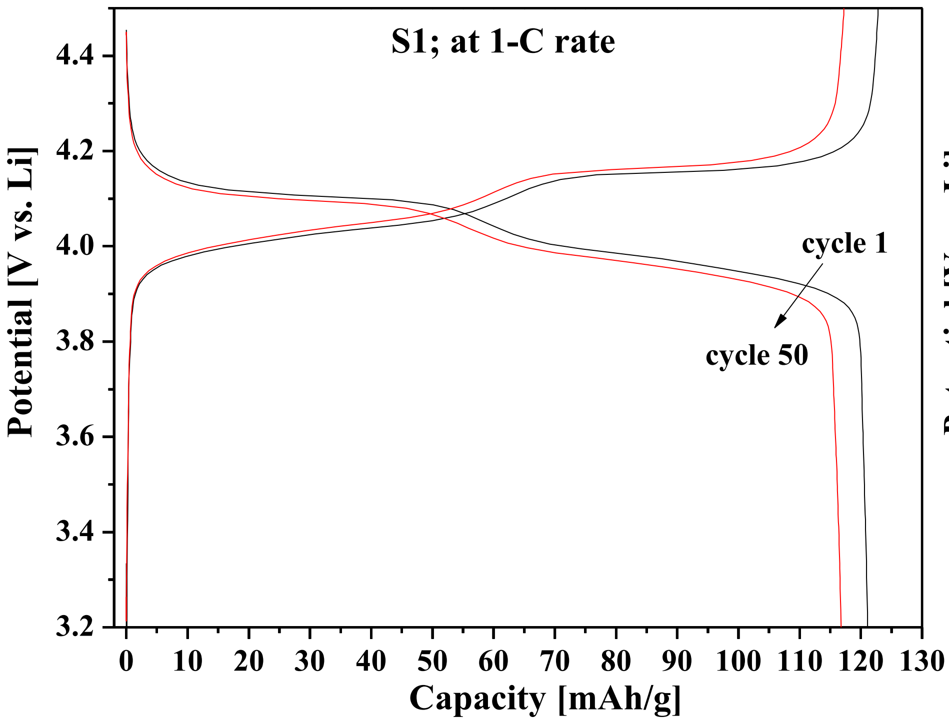

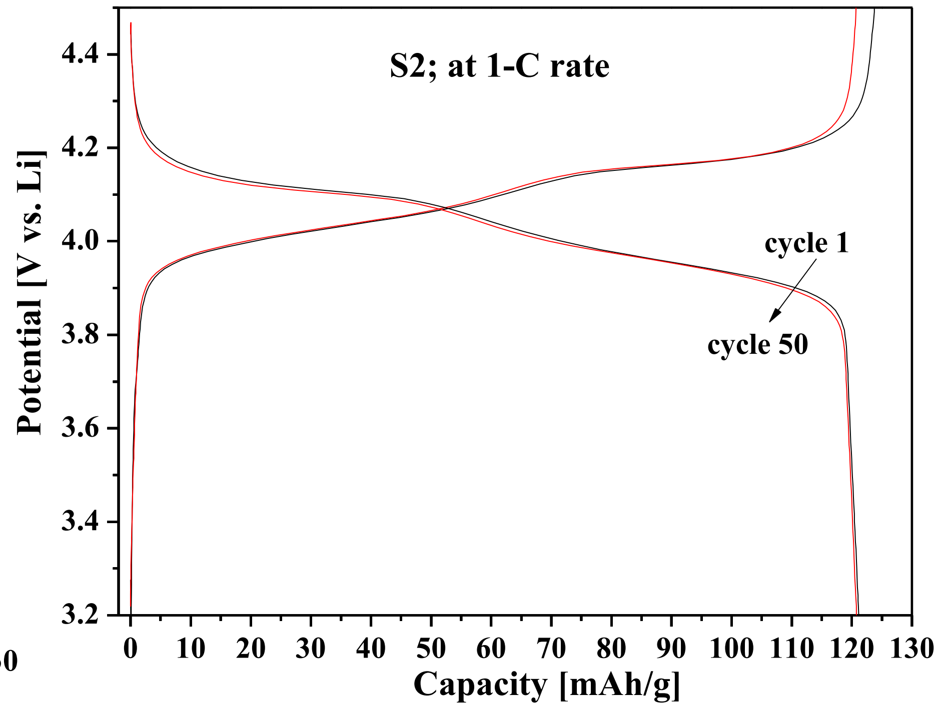

Figure S14. Charge-discharge curves at 1-C rate.

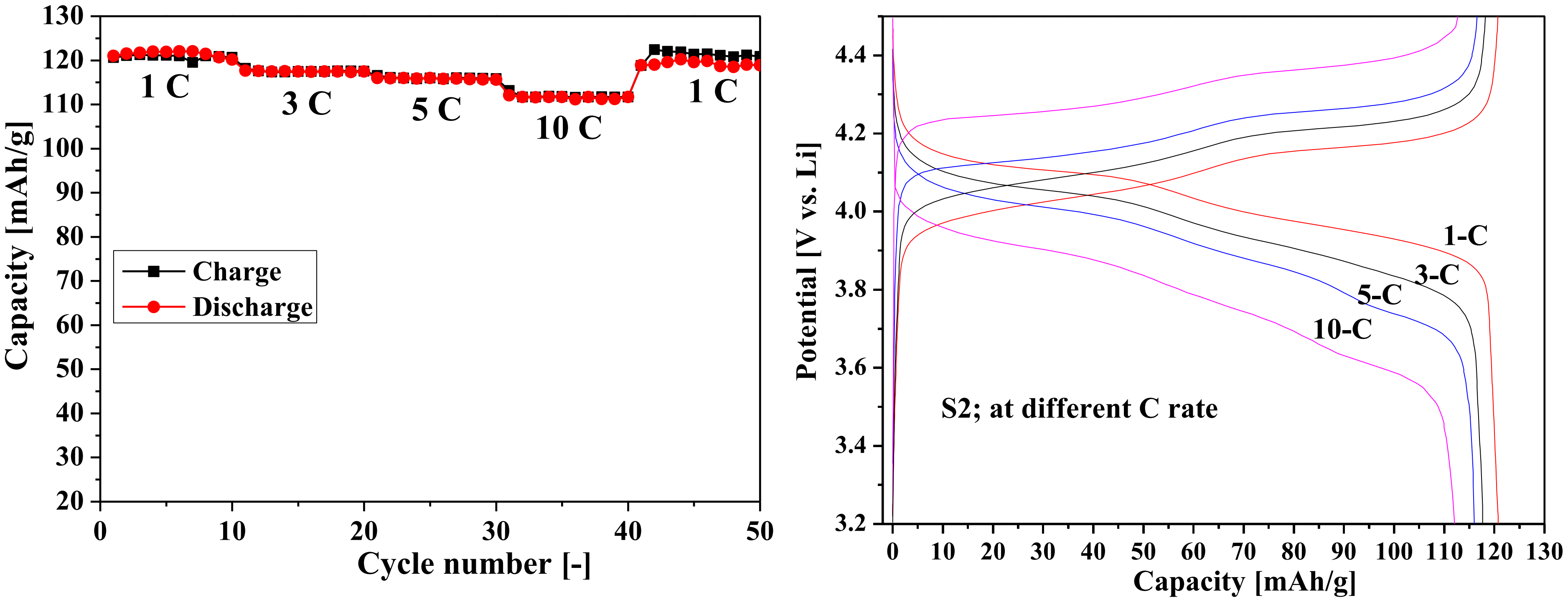

Figure S15. Cycling performance and the charge-discharge curves for the porous $LiMn_2O_4$ hollow spheres (S2) at different C-rates.